

IN SILICO INHIBITOR DESIGN FOR MONOAMINE
OXIDASE A AND B ISOZYMES

ÇAĞLA MIDİK

20091109006



Kadir Has University

2012

IN SILICO INHIBITOR DESIGN FOR MONOAMINE OXIDASE A
AND B ISOZYMES

ÇAĞLA MIDİK

Computational Biology and Bioinformatics, Kadir Has University, 2012

Submitted to the Graduate School of Science Institute
in partial fulfillment of the requirements for the degree of
Master of Science
in
Computational Biology and Bioinformatic

KADIR HAS UNIVERSITY

2012

KADIR HAS UNIVERSITY
GRADUATE SCHOOL OF SCIENCE AND ENGINEERING

MONOAMINE OXIDASE ISOZYMES LIGAND DESIGN

ÇAĞLA MIDİK

APPROVED BY:

| | | |
|---------------------|------------------------|-------|
| ... | (Kadir Has University) | |
| (Thesis Supervisor) | | |
| ... | (Marmara University) | |
| ... | (Kadir Has University) | |
| ... | (Kadir Has University) | |

APPROVAL DATE:

Abstract

In this thesis study, MAO-A and MAO-B isozymes are selected as target enzymes that have important role of regulation of diseases such as ‘‘Parkinson, Alzheimer and depression’’. MAO isozymes which catalyze the oxidation of monoamines in the body stand out in these diseases. Today explicitly known that MAO enzymes oxidize the neurological amines such as serotonin, dopamine, neuroadrenaline more than usual way and result in the reduction of the level of these important monoamines creating disease state.

Three-dimensional structures of cloned human MAO-A complexed with harmine ligand (2z5x) and human MAO-B complexed with safinamide (2v5z) are taken from protein data bank. Both isoforms contain flavin molecule as cofactors.

Taking into consideration of the previous studies, 210 new ligands are created. Of these ligands 105 are the R stereoisomers and the other 105 are S stereoisomers.

The objective of this study is to use computer-aided drug design (CADD) methods based on structure-based drug design. As a result we obtained the best orientation of these ligands in the active site of both isozymes. Using of improved docking methods the lowest possible binding energy and the poses of the ligands in the enzyme complex are scored.

Docking programs exploit their own scoring functions by specific algorithms. Hereby, binding energies of target enzyme and ligands are estimated at the lowest energy conformations by these scoring functions. In this study, docking simulations are performed by Autodock 4.2 and Accelrys 3.1 libdock programs.

Evaluation of docking studies by Autodock 4.2. suggested us the results generated are very reasonable K_i values. The results of both docking simulation methods showed us the ligands 1d3r, 1a3r and 1a6r are effectively inhibit MAO-A isozyme whereas ligands 2d1r, 1d6s, 1d3s and 3b4r selectively inhibit MAO-B

isozyme. In conclusion, these inhibitors are very important candidates for MAO enzyme and may lead the future studies.

Özet

Bu tez çalışmasında ‘‘Parkinson, Alzheimer ve Depresyon’’ gibi hastalıkların meydana gelmesinde önemli rol oynayan MAO enziminin iki izomeri olan MAO-A ve MAO-B izoenzimleri hedef olarak seçilmiştir. Vücuttaki monoaminleri katalize etmekle görevli olan MAO izoenzimleri özellikle bu hastalıklarda göze çarpmaktadır. Bu hastalarda normalden daha fazla çalışarak vücuttaki serotonin, dopamin, nöradrenalin gibi monoaminlerin konsantrasyonunu oldukça düşürdükleri günümüzde açıkça bilinmektedir.

Flavin ailesi üyesi olan bu enzimlerin kristalize edilmiş üç boyutlu yapıları insan MAO-A’sı harmine kompleksi ile (2z5x), insan MAO-B’si ise safinamide kompleksiyle (2v5z) birlikte olmak üzere protein bilgi bankasından alınmıştır.

Daha önceki bilimsel çalışmalar göz önünde bulundurularak MAO izoenzimlerinin inhibisyonuna yönelik 105’i r-stereo izomeri, 105’i s-stereo izomeri olmak üzere toplam 210 tane ligant bileşiği oluşturulmuştur Bilgisayar destekli yapıya dayalı ilaç tasarımı, enzimlerin aktif bölgesi ile ligantlar arasındaki en düşük enerji konformasyonlarında bağlanma durumlarını ölçmeyi hedefler. Bunu yaparken geliştirilmiş docking metotlarını kullanarak enzimlerin ve ligantların 3 boyutlu yapılarındaki değişkenliklerini de hesaba katar.

Bilgisayar destekli docking araçları spesifik algoritmaları sayesinde kendi skor fonksiyonlarını üretir. Böylelikle ligantların hedef enzime en düşük konformasyonda bağlanma enerjileri bu skorlar yardımıyla tahmin edilmektedir.. Yaptığımız çalışmada docking simülasyonları Autodock 4.2 ve Accelryss 3.1 libdock programları ile gerçekleştirildi.

Autodock 4.2 programıyla yapılan çalışmalar sonunda ölçülen Ki değerleri olumlu sonuçlar vermiştir. Ayrıca her iki docking simülasyonunda incelenen ligant bileşikleri 1d3r,1a3r,1a6r MAO-A izoenzimiyle eşleşmede ve 2d1r, 1d6s, 1d3s ve 3b4r ligant bileşikleri ise MAO-B izoenzimiyle eşleşmede oldukça yüksek sonuçlar

vermiştir. Bu ligantlar MAO enzimleri için inhibitör adayları olduklarını gösterirler ve gelecek çalışmalara ışık tutabilirler.

Acknowledgements

It is a pleasure to thank the many people who made this thesis possible. There are many people who helped to make my years at the graduate school most valuable.

First and most importantly, I want to thank the best educator ever I seen, my major professor and dissertation supervisor Prof. Dr. Kemal Yelekçi and his guidance for his unlimited support, endless patience throughout my thesis studies. It has been an honor and privilege working with him over years.

I also thank Assist Prof. Demet Akten Akdoğan and Dr. Tuğba Arzu Özal who contributed much to improve of my dissertation work.

My special thanks go to friends, Filiz Varnalı, Jale Güler, Levent Binnetoğlu, Erçin Dinçer, Seda Demirci, Sibel Çakan and Gizem Tatar who helped me me all through the years full of class work and exams for their supporting during my thesis.

I want to thank Nurdan Kayrak and Bora Büyüktürk who contributed my studies.

The last words go to my fragmented family. Big thanks go to my parents Berrin Karakaş, Battal Mıdık and my brother N. Serhat Mıdık for their all supports and I thank my dear engaged Mihrace İnel, for her endless support through this long journey.

Table of Contents

| | |
|---|------|
| Abstract | ii |
| Özet | iv |
| Acknowledgements | i |
| Table of Contents | ii |
| List of Tables..... | iv |
| List of Figures | v |
| List of Symbols | vii |
| List of Abbreviations..... | viii |
| 1. Introduction | 1 |
| 2. Background of Monoamine Oxidase..... | 3 |
| 2.1. Introduction of Monoamine Oxidase | 3 |
| 2.1.1. Comparing of Monoamine Oxidase Isozymes | 4 |
| 2.1.2. Active site of Monoamine Oxidase | 5 |
| 2.1.3. Amines of Monoamine Oxidase Catalyze..... | 7 |
| 2.1.3.1 Dopamine | 7 |
| 2.1.3.2. Serotonin..... | 8 |
| 2.1.3.3. Ephinephrine | 9 |
| 2.1.3.4. Norepinephrine | 9 |
| 2.2. Mechanism of Monoamine Oxidases Amine Catalyze | 10 |
| 2.3. Background of Known MAO Inhibitors | 12 |
| 3. Materials and Methods | 14 |
| 3.1.1. General Properties of Molecular Docking | 14 |
| 3.1.2. General Properties of AUTODOCK | 15 |
| 3.1.3. General Properties of Accelrys Discovery Studio | 17 |
| 3.2. Preparing Compounds | 18 |
| 3.2.1. Preparing Monoamine Oxidase Isozymes..... | 18 |
| 3.2.2. Preparing Ligands of Monoamine Oxidase Isozymes..... | 19 |
| 3.3. Molecular Docking..... | 22 |
| 3.3.1. Docking Setup of AUTODOCK 4.2 | 22 |
| 3.3.2 Enzyme-Ligand Molecule Docking by AUTODOCK 4.2..... | 23 |
| 3.3.3 Docking Setup of LIBDOCK | 24 |
| 4. Result and Discussion | 25 |
| 4.1. Results of Molecular Docking Studies by Autodock 4.2 | 25 |
| 4.2. Results of Molecular Docking Studies by LIBDOCK | 27 |

| | |
|---|----|
| 4.3. Analysis of Monoamine Oxidase A – Ligand Docking | 28 |
| 4.4. Analyses of Monoamine Oxidase B - Ligand Docking | 36 |
| Conclusions | 47 |
| APPENDIX A: PARAMETER FILES of AUTODOCK 4.2 STUDIES | 51 |
| APPENDIX B: RESULTS of AUTODOCK 4.2 DOCKING DATA | 57 |
| Bibliography | 63 |
| Curriculum Vitae | 68 |

List of Tables

| | |
|-----------|---|
| Table 3.1 | Experimental details of Human Monoamine Oxidase A with harmine (Journal: (2008) Proc.Natl.Acad.Sci.Usa 105: 5739-5744). |
| Table 3.2 | Experimental details of Human Monoamine Oxidase B with the selective inhibitor safinamide (Journal: (2007) J.Med.Chem. 50: 5848). |
| Table 3.3 | Preparing code names of ligands. |
| Table 4.1 | Top 20 Autodock docking results of MAO-A and MAO-B isozymes. |
| Table 4.2 | Results of Libdock docking for MAO-A and MAO-B isozymes. |
| Table 4.3 | 2-D pictures of the ligands interaction by MAO-A at the lowest docking energy conformation. |
| Table 4.4 | 2-D pictures of the ligands interaction by MAO-A at the lowest docking energy conformation. |
| Table 5.1 | 2-D chemical structures and detailed docking results of MAO-A and MAO-B ligand candidates. |

List of Figures

- Figure 2.1. 3-D crystal structures of human MAO-A in complex with harmine. (a) display style is solid ribbon.(b) display style is lines and balls represent FAD.
- Figure 2.2. 3-D crystal structure of MAO-B in complex with the selective inhibitor safinamide.(a) display style is solid ribbon. (b) display style is lines and balls represent FAD.
- Figure 2.3. Comparing 3-D structures of MAO-A & MAO-B isozymes.
- Figure 2.4. (A) Chemical structure of FAD.(B) Active site comparison of human MAO-A and human MAO-B.(C) The active site cavity (red surface) of MAO-B in Complex with deprenyl (black) is depicted (NCBI)
- Figure 2.5. 2-D chemical structure of FAD in active side of MAO-A & MAO-B.
- Figure 2.6. 2-D chemical structure of dopamine.
- Figure 2.7. 2-D chemical structure of serotonin.
- Figure 2.8. 2-D chemical structure of ephinephrine (adrenaline).
- Figure 2.9. 2-D chemical structure of noradrenaline or (R)-(-)-norepinephrine.
- Figure 2.10. Figure 2.10. Steps of the oxidative deamination of amines catalyzed by MAO.(a) FAD reduction.(b) represent deamination (c)represent FAD redoxidation.
- Figure 2.11. 2-D chemical structure of hydride mechanism.
- Figure 2.12. Mechanism of single electron transfer (SET).
- Figure 2.13. 2-D chemical structure of iproniazid.
- Figure 2.14. 2-D chemical structure of moclobemide.
- Figure 3.1. Workflow of docking studies.
- Figure 3.2. 2-D chemical structure of ligand scaffold.
- Figure 3.3. 2-D view of ligand scaffold by Accelrys Discovery Studio 3.1.
- Figure 3.4. Preparing code names of ligands.
- Figure 4.1. 3-D view of ligand 1d3r and active side of MAO-A at the lowest energy conformation.

- Figure 4.2. 3-D view of ligand 1d6r and active side of MAO-A at the lowest energy conformation.
- Figure 4.3. 3-D view of ligand 1a3r and active side of MAO-A at the lowest energy conformation.
- Figure 4.4. 3-D view of ligand 1d1r and active side of MAO-A at the lowest energy conformation.
- Figure 4.5. 3-D view of ligand 1a6r and active side of MAO-A at the lowest energy conformation.
- Figure 4.6. 3-D view of ligand 1c3r and active side of MAO-A at the lowest energy conformation.
- Figure 4.7. 3-D view of ligand 1c6r and active side of MAO-A at the lowest energy conformation.
- Figure 4.8. 3-D view of ligand 3e6r and active side of MAO-A at the lowest energy conformation.
- Figure 4.9. 3-D view of ligand 2c7s and active side of MAO-A at the lowest energy conformation.
- Figure 4.10. 3-D view of ligand 1d7s and active side of MAO-A at the lowest energy conformation.
- Figure 4.11. 3-D view of ligand 2d1r and active side of MAO-B at the lowest energy conformation.
- Figure 4.12. 3-D view of ligand 1d4s and active side of MAO-B at the lowest energy conformation.
- Figure 4.13. 3-D view of ligand 1d5s and active side of MAO-B at the lowest energy conformation.
- Figure 4.14. 3-D view of ligand 1d6s and active side of MAO-B at the lowest energy conformation.
- Figure 4.15. 3-D view of ligand 1d3s and active side of MAO-B at the lowest energy conformation.
- Figure 4.16. 3-D view of ligand 1a3s and active side of MAO-B at the lowest energy conformation.
- Figure 4.17. 3-D view of ligand 1a1s and active side of MAO-B at the lowest energy conformation.
- Figure 4.18. 3-D view of ligand 3b4r and active side of MAO-B at the lowest energy conformation.
- Figure 4.19. 3-D view of ligand 1c6s and active side of MAO-B at the lowest energy conformation.
- Figure 4.20. 3-D view of ligand 3d4s and active side of MAO-B at the lowest energy conformation.
- Figure 5.1. Detailed docking results and chemical structures of MAO-A and MAO-B inhibitor candidates.

List of Symbols

| | |
|--------------|--|
| Å: | Angstrom |
| α : | Alpa angle |
| β : | Beta angle |
| γ : | Gama angle |
| ΔS : | Entropy lost upon binding |
| R: | Point of benzoic ring |
| R1: | Name of a benzoic ring |
| R2: | Name of a benzoic ring |
| g: | Gram |
| L: | Ligand |
| P: | Protein |
| E: | Enzyme |
| W: | Constant |
| V: | Volume of atoms |
| S: | Solvation patameter |
| Dij: | Maximal well depth for hydrogen bonds, oxygen and nitrogen |
| Cij: | Maximal well depth for hydrogen bonds, oxygen and nitrogen |
| -R: | Right isomer |
| -S: | Left isomer |
| pM: | Picomolar |
| nM: | Nanomolar |
| μ M: | Micromolar |
| Obs: | Observed structure factors |

List of Abbreviations

| | |
|---------------------|-------------------------------------|
| MAO: | Monoamine oxidase |
| MAO-A: | Monoamine oxidase – A |
| MAO-B: | Monoamine oxidase – B |
| FAD: | Flavine di nucleotide |
| π -interaciton: | A type of non-covalent interaction |
| X-RAY: | A form of electromagnetic radiation |
| 3-D: | Three dimension |
| SET: | Single electron transfer |
| GA: | Genetic algorithm |
| LGA: | Lamarcian genetic algorithm |
| SASA: | Solvent accessible solvent area |
| GPF: | Grid parameter file |
| DPF: | Docking parameter file |
| VDW: | Van der waals |
| NMR: | Nuclear magnetic resonans |
| SSRI: | Selective serotonin inhibitors |
| Hbond: | Hydrogen bond |
| Tor: | Torsion |
| Sol: | Desolvation |
| Elec: | Electrostatic |
| Ala: | Alanine |
| Arg: | Arginine |
| Asn: | Asparagine |
| Asp: | Aspartic acid |
| Cys: | Cysteine |
| Glu: | Glutamic acid |
| Gln: | Glutamine |
| Gly: | Glycine |
| His: | Histidine |
| Hyp: | Hydroxyproline |
| Ile: | Isoleucine |

| | |
|------|---------------|
| Leu: | Leucine |
| Lys: | Lysine |
| Met: | Methionine |
| Phe: | Phenylalanine |
| Pro: | Proline |
| Glp: | Pyroglutamic |
| Ser: | Serine |
| Thr: | Threonine |
| Trp: | Tryptophan |
| Tyr: | Tyrosine |
| Val: | Valine |

Chapter 1

1. Introduction

Monoamine oxidase enzymes are classified as flavoproteins because they include flavine adenine dinucleotide (FAD). In most cell type, MAO is observed at the mitochondrial outer membrane. MAO includes two different isoforms such as MAO-A isozyme and MAO-B isozyme. Both isozymes found in brain but also reside in different kinds of cell. MAO-A is generally observed in catecholaminergic neurons whilst MAO-B is found in serotonergic neurons also both of these isozymes accessible in the astroglial cell [1].

MAO plays so crucial role in the mammalian body system cause of catalyze oxidation of monoamines. Even amino acid sequences of MAO isozymes %70 similar, they are encoded from separate genes and they have been identified by their substrate selectivity and their inhibitor sensitivity [2]. General view, MAO-A selectivity inhibitor is clorgline and selectivity substrate serotonin while MAO-B selectivity inhibitor is R-deprenyle and selectivity substrate is dopamine [3]. Both isozymes play active role for deamination of dopamine, tyramine and tryptamine. According to Edmonson [4] MAO-A preferable deaminates aromatic monoamines for instance the neurotransmitters serotonin, adrenaline. On the other hand MAO-B generally oxidazes β -phenylethylamines and benzylamines.

Present, close relation between neurotransmitter amines and such diseases is evidenced by chemical, biological computations, pharmaceutical studies and clinical researches. Especially, after the discovery of X-RAY crystallography enabled proteins virtual visualization so vast data of compound which related structure of proteins are accessible for novel drug design and developing of medicinal industry. According to Yelekçi [5] after the specification of the 3-D crystal structure of MAO-B pave the way for development of computer-assisted more selective and reversible inhibitor design.

In the major depression diseases, deficit of monoamines is observed basically neuroepinephrine and serotonin where critical synapses in the central nervous

system [6]. In the Parkinson diseases, concentration of dopamine is decreased. Consideration of MAO deamination function of monoamines, these results shows that MAO inhibitors have critical role in the therapy of severe neurological and psychological disorders. Combinational chemistry offers vast data about new molecule compounds so clearly known that experimental studies of novel drug design lead to time-consuming and loss of money.

In this thesis, chapter 2 provides detailed information of MAO isozymes, their function mechanisms and amines which are catalyzed by MAO. Also comparison of MAO-A and MAO-B isozymes is presented. In the chapter 3, two main target enzymes are prepared that are MAO-A, MAO-B isozymes and 210 many designed inhibitor (which are includes both of -R and -S stereoisomers) candidates are created by considered to previous MAO inhibition study literature. Also information of molecular docking tools is given and their parameters are set up. Finally results of docking studies, detailed analysis of ligand candidates and discussion are given in chapter 4.

Aim of in this thesis studies is designing of inhibitor candidates and finding the best MAO-A and MAO-B inhibitors by using the automated docking tools. Results of this thesis can help for the next studies for treatment of Parkinson, Alzheimer and depression diseases.

Chapter 2

2. Background of Monoamine Oxidase

2.1. Introduction of Monoamine Oxidase

MAO is a flavo protein situated at the mitochondria's outer membrane of neural, glial and other cells, specially appertain in the brain and liver. MAO enzyme has an important role in some psychiatric and neurological disorders, including depression and Parkinson's disease because inhibition of MAO increases the concentration of neurotransmitters in the central nervous system, searching for the effective inhibitors represent one significant approach to thriving novel drugs to treat such diseases [7]. Enzyme of MAO was discovered in liver as tyramine oxidase by Mary Bernheim in 1928.

After the 1950's, MAO inhibitors were thought for clinical treatments but using with other type drugs and nutrients that including tyramine was caused a significant risk of rapid increased blood pressure (hypertensive crise) and other different side effects. Thus, developments of therapeutic monoamine oxidase inhibitors are regressed. With the discovery of human monoamine oxidase's two isoforms crystal structure which called monoamine oxidase A (Mao A) and monoamine oxidase B (Mao B), Protein – ligand selectivity interactions and **catalytic** mechanisms better understood.

Today, vast number compounds are examining by the development of computational chemistry and computer-aid bioinformatics. After the determination of three dimensional crystalized structures of MAO isozymes by X-RAY crystallography and NMR, in last decade found in the literature has increased a great deal of space. Also over the therapeutic potency of rational selectivity enzymes, lot of research has been done.

2.1.1. Comparing of Monoamine Oxidase Isozymes

MAO-A and MAO-B have own specific substrates in addition they have own specific inhibitors too. MAO-A is mostly located at the catecholaminergic neurons, and MAO-B is located at serotonergic neurons and glia [8].

Simply MAO-A oxidizes serotone and noradrenaline while MAO-B oxidizes dopamine and phenylethylamine. Monoamine oxidases isozymes (MAO-A and MAO-B) have about % 70 amino acid sequence similarity [9]. Human MAO-A has 59.700 molecular weight and human MAO-B has 58.800 molecular weight.

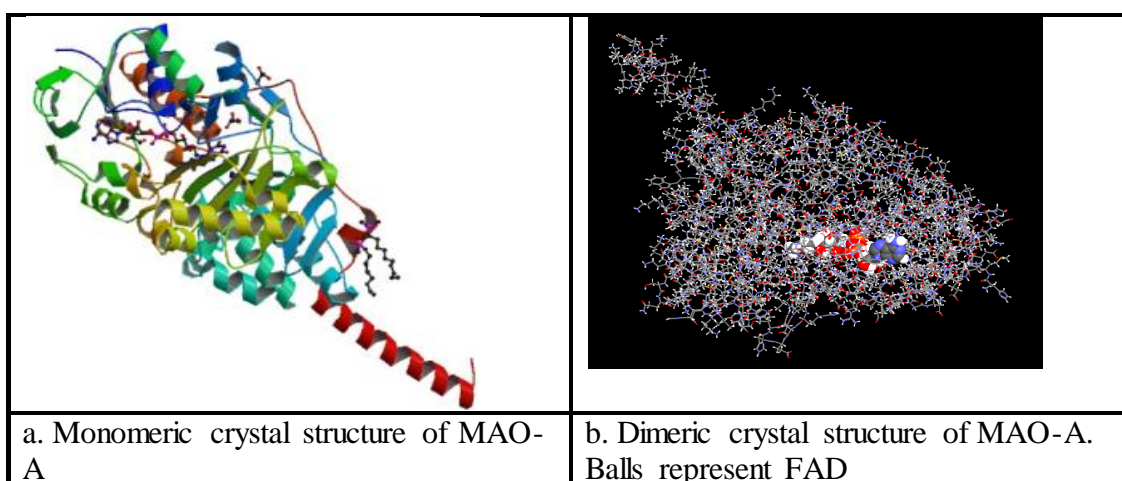


Figure 2.1. 3-D crystal structures of human MAO-A in complex with harmine. on the figure a. and on the figure b.

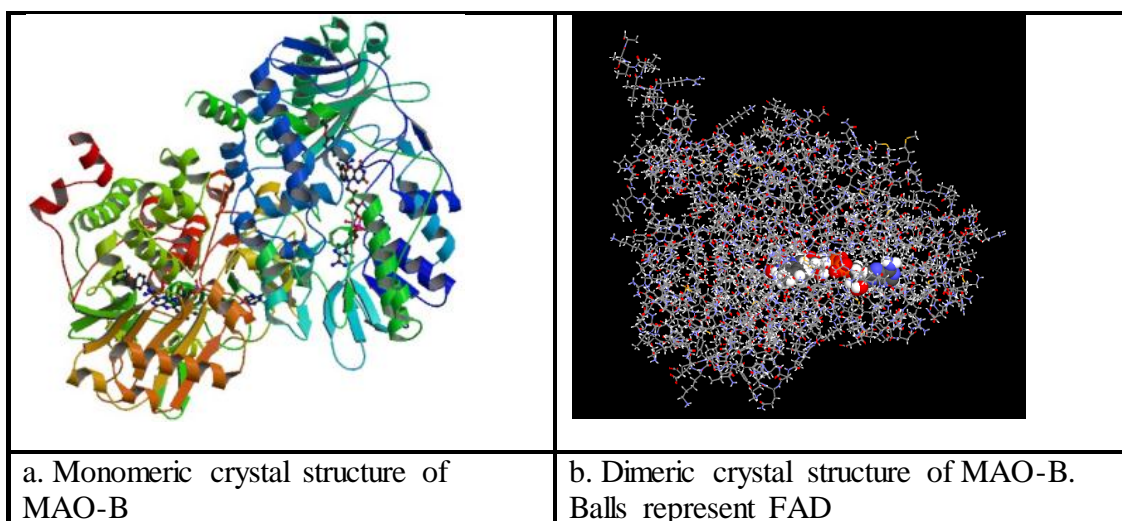


Figure 2.2. 3-D crystal structure of MAO-B in complex with the selective inhibitor safinamide

MAO-A and MAO-B isozymes are compared with the software programs Blast2 and Fatcat. Blast2 software program displays the similarity of sequence alignments and as a result calculating of pairwise sequence alignments display that specially % 68 identities, % 81 positives sings for MAO-A and MAO-B isozymes.

On the other hand comparing of MAO-A and MAO-B isozymes by the Fatcat program displays that their 3-D structures have high degree similarity as figure 2.3

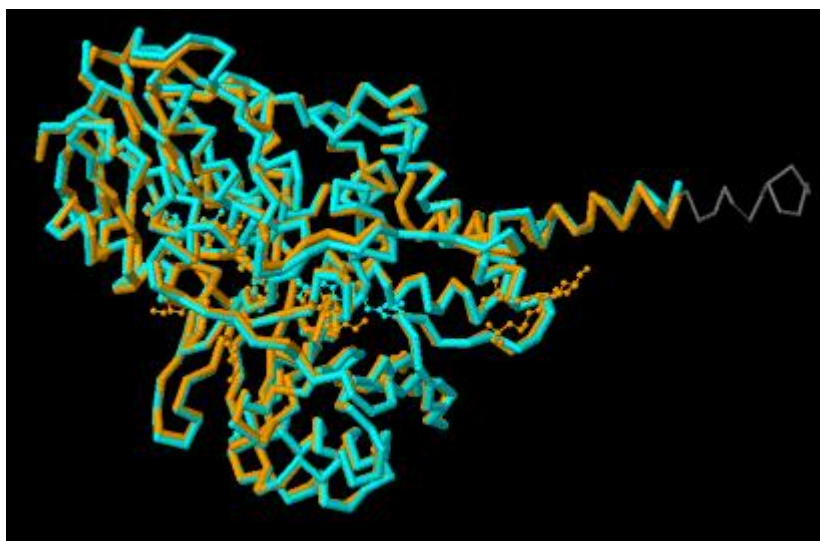


Figure2.3. Comparing 3-D structures of MAO-A isozyme & Mao-B isozyme. Orange color represent the Mao-A and turquoise color represent the Mao-B

2.1.2. Active site of Monoamine Oxidase

In the enzymes, the area that includes catalytic residues, makes binding the substrate, in this way actualizes the reaction is known as the active site. Monoamine oxidases contain the covalent bound cofactor flavine adenine dinucleotide (FAD) in the active site. The FAD is bound to the protein in an extended conformation with the most of the bonds to the protein detected as hydrogen bonds with amino acid side chains, amide bonds, and water molecules. Since those amino acids interacting with the FAD are conserved in MAO-A, it is proposed that the FAD binding site in MAO-A is quite similar to that in MAO-B. According to Edmonson et al [10] comparing active side of MAO-A (human) and MAO-B (human) is illustrated as Figure 2.4.

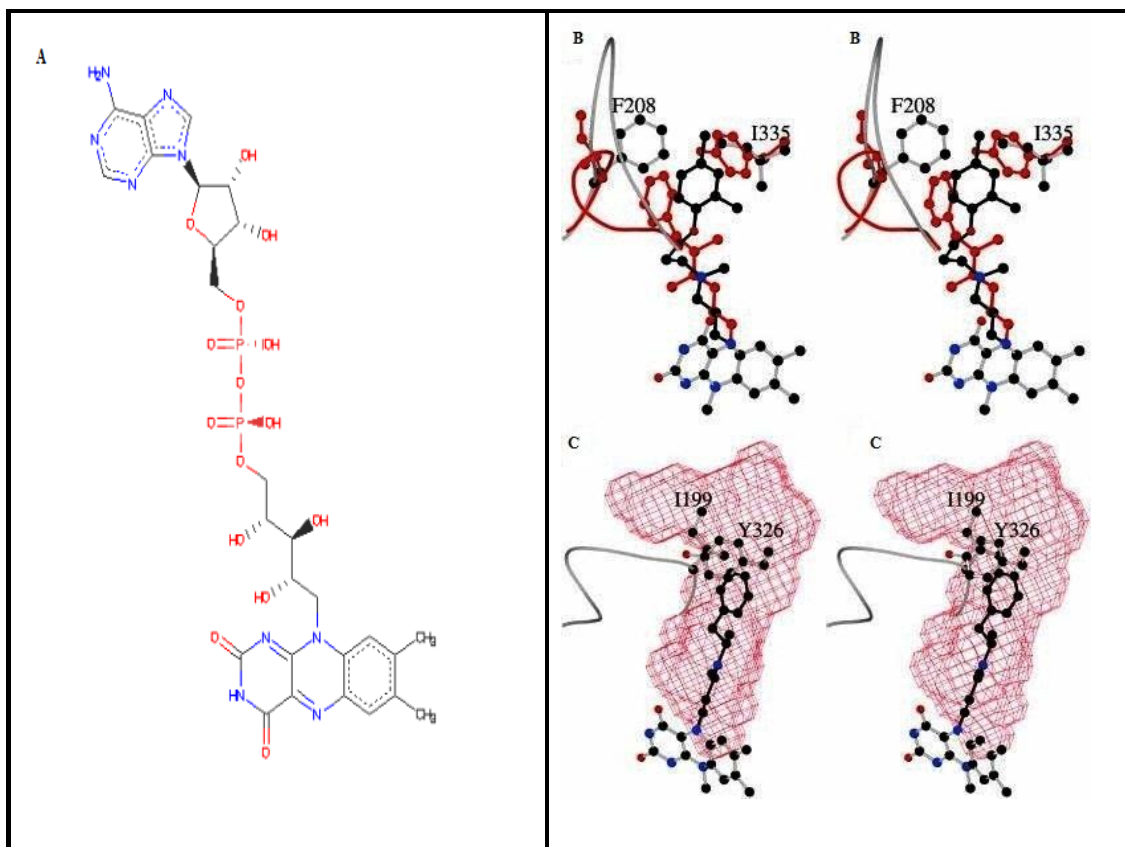


Figure 2.4. (A) Chemical structure of FAD that is located at the active side of MAO. B and C figures are taken from national center for biotechnology information.

On the figure 2.4(B) indicate that active site comparing of human MAO-A and human MAO-B with the critical Phe-208 and Ile-335 residues of MAO-A superimposed to the correspondent residues of MAO-B such as Ile-199 and Tyr-326. Atoms of inhibitor and protein molecules of MAO-B are shown in the red cage. According to A, the pattern has been rotated by $\approx 90^\circ$ around the vertical axis in the plane of the model. On the figure 2.4(C) represent that the active site cavern (red surface) of MAO-B in complex with deprenyl (black) is shown.

Flavin di nucleotide that is depended to a cysteine amino acid residue of Mao's 8α position with covalent bind as figure 2.5.

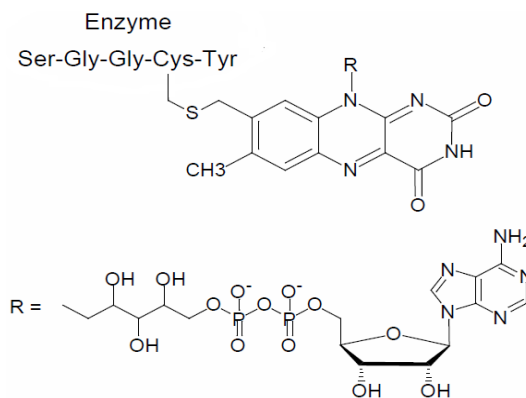


Figure 2.5. 2-D chemical structure of FAD in active side of MAO-A & MAO-B

2.1.3. Amines of Monoamine Oxidase Catalyze

2.1.3.1 Dopamine

Dopamine is a type of the catecholamine neurotransmitters that accessible in the brain. It is derived from tyrosine and is the precursor to neurepinephrine and epinephrine. Dopamine has important role in the many cerebrum processes that movement of control, emotional and mental response, and ability to experience delight and ache. In the respect of chemical, molecular formula is $C_8H_{11}NO_2$ and molecular weight is 153.17844 [11].

Regulation of dopamine has critical role in human intellectual and physical health. Neurons which including the neurotransmitter dopamine are clustered in the midbrain in an area called the substantia nigra, especially in disease of Parkinson, the dopamine- transmitting neurons die in this area. [12]. Eventual, brains of patients with disease of Parkinson do not include almost any dopamine.

Two major degradation pathways for dopamine exist. In most areas of the brain, including the striatum and basal ganglia, dopamine is inactivated by reuptake via the dopamine transporter, then enzymatic breakdown by monoamine oxidase into 3,4-dihydroxyphenylacetic acid [13].

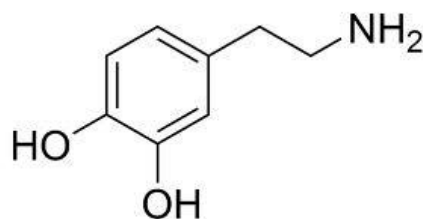


Figure 2.6. 2-D chemical structure of dopamine

2.1.3.2. Serotonin

Serotonine (5-hydroxytryptamine 5HT) is firstly observed in the gastrointestinal tract, platelets and nervous system of human [14]. Serotonine's molecular formula is known as C₁₀H₁₂N₂O and molar mass is measured 176.215 g/mol and slightly soluble in the water. The functions of serotonin are in large quantities and appear to involve control of regulating appetite, dexterity of learning and memory, temperature regulation, state of mind, behavior (including sexual and hallucinogenic behavior), cardiovascular function, muscle contraction, endocrine regulation, and depression.

Lately, selective serotonin inhibitors (SSRIs) are preferred and used for treatment of suppress depression diseases. These drugs process by altering the function of neurons that release serotonin by blocking the reuptake of serotonin back into the cell. Thus the concentration level of serotonin efficiency is increased in any where of the nervous system that make uses this neurotransmitter as a chemical signal between cell transmission mechanism. The SSRIs are improved into the drug of preference because they present lesser side effects due to their limited action to reuptake serotonin alone and no other neurotransmitters [15].

Serotonin synthesis occurs in a several process first step of that begins with the amino acid tryptophan. The second step in serotonin production includes an enzyme named tryptophan hydroxylase. Tryptophan hydroxylase appends a hydroxyl group to tryptophan, generating 5-hydroxytryptophan. Another enzyme, amino acid decarboxylase, eliminates a carboxyl group from 5-hydroxytryptophan, leaving 5-hydroxytryptamine, or serotonin. Then the serotonin is inactivated by a MAO. MAO degrades serotonin by cleaving the amine group off, which is the deamination

reaction. The two products are ammonium ion and 5-hydroxyindole-3-acetaldehyde, this essentially leaves the neurotransmitter deactivated [16].

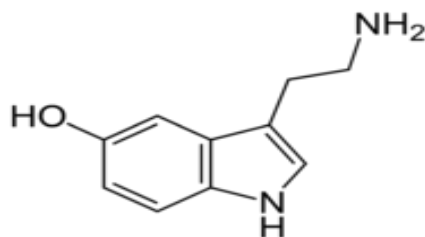


Figure 2.7. 2-D chemical structure of serotonin

2.1.3.3. Ephinephrine

Ephinephrine (adrenaline) plays role as a hormone and plays role as a neurotransmitter. It responsible for increasing heart rate, constricts blood vessels, dilates air passages and participates in the fight-or-flight response of the sympathetic nervous system [17]. The significant physiological triggers of ephinephrine release center upon stresses, such as physical threat, enthusiasm, loudness, bright lights, and high environment temperature [18]. Chemically, epinephrine is a catecholamine and further only the adrenal glands from the amino acids tyrosine and phenylalanine produce as a monoamine.

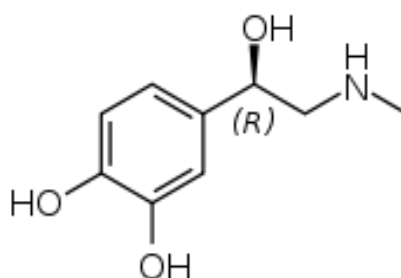


Figure 2.8. 2-D chemical structure of ephinephrine (adrenaline)

2.1.3.4. Norepinephrine

Norepinephrine consists of a catecholamine and a phenethylamine. The inherent stereoisomer is *L*-(-) - (*R*) - norepinephrine. This monoamine has an

important role of brain's notice and response stimulations. Noradrenaline's molecular formula is $C_8H_{11}NO_3$ and molecular weight is $169.18 \text{ g mol}^{-1}$ [19].

A major important function of norepinephrine is its role as the neurotransmitter released from the sympathetic neurons affecting the heart. Enhance in norepinephrine from the sympathetic nervous system leads to increasing the rate of contractions [20].

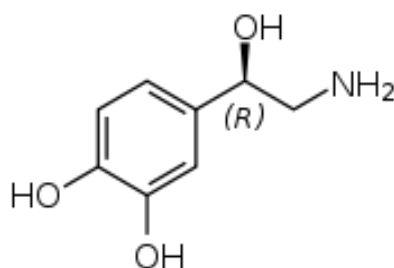


Figure 2.9. 2-D chemical structure of noradrenaline or (R)-(-)-norepinephrine

2.2. Mechanism of Monoamine Oxidases Amine Catalyze

Monoamine oxidase is a flavin-dependent enzyme that catalyzes the oxidative deamination of a variety of amine neurotransmitters and toxic amines, to the corresponding imines which are nonenzymatically hydrolyzed to aldehydes [21]. The cofactor FAD plays active role in the reaction. This could be schematized in three steps which are same for both enzymes as figure 2.10.

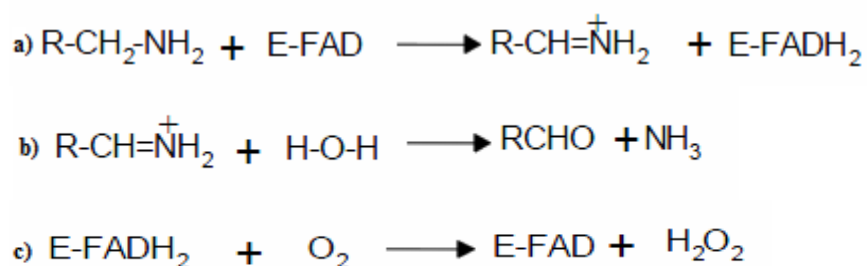


Figure 2.10. Steps of the oxidative deamination of amines catalyzed by MAO.(a) represent FAD reduction.(b) represent deamination.(c) represent FAD reoxidation

As a result of enzymatic reaction, aldehyde derives from imine by water. Reduced FAD is oxidized by aid of molecular oxygen and returns to form of before reaction as catalyzer.

Various mechanisms are proposed for the oxidation of the biological amines by monoamine oxidases. According to Yelekci these mechanisms are handled in four section such as Two Electron Mechanism, Carbanion Followed by One-Electron Transfers, One-Electron Mechanism Hydride Mechanism [22].

According to Hydride Mechanism, amine α -H is transported to Flavine as Hydride. Thence two electrons and one proton are transferred to the flavine so reaction is completed but hydride transfer requires high energy and this causes some questions about Hydride Mechanism [23].

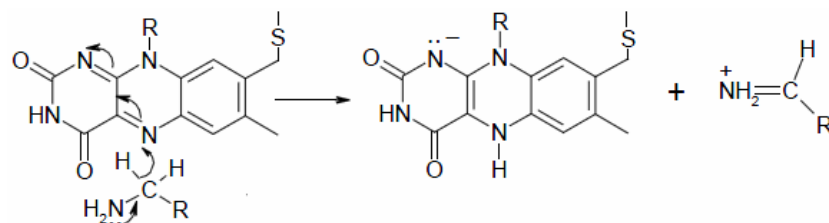


Figure 2.11. 2-D chemical structure of hydride mechanism.

According to suppose of Silverman, one electron flavin mechanism is possible for both monoamine oxidase isozymes, α -carbon oxidation of amines begins by the one electron transfer. One electron of the unmatched electron pairs where located nitrogen atom of the monoamine (a) is transferred to the flavine thus radical amine cation (b) and FADH occur. After the leaving hydrogen of α -Carbon where located radical amine cation, by the path of "1" compound transforms to α -radical amine (c). In this situation reaction can follow two different path as "2" or "3". If reaction continues according to path "2" second electron could transfers to FADH, can formation of iminium ion (e). On the other hand if reaction proceed pursuant to path "3" could radical combine with a radical that located other regions of enzyme so does covalent bounding by X and transforms to compound (d). If this consisting intermediate product can be stable enough that can make the enzyme inactive and then it transforms iminium ion (e) and free enzyme [24].

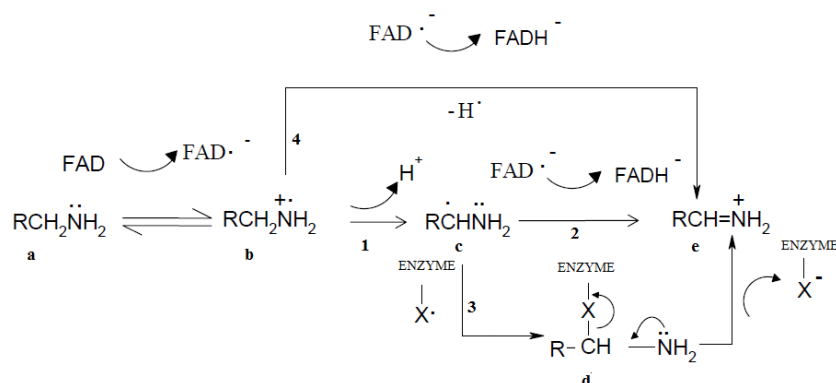


Figure 2.12. Mechanism of single electron transfer (SET)

In the disease of depression concentration of amines neurotransmitters such as serotonin, dopamine decreases. Important involved enzyme of these amines that monoamine oxidase is considered for target enzyme for depression disease

2.3. Background of Known MAO Inhibitors

A great number of studies for inhibition of MAO are inspired from old inhibitors such as Moclobemide, Iproniazid.

First potent MAO inhibitor is Iproniazid that was introduced in therapy of depression disease, in 1957. Its side effects with other chemicals and particular nutrients, the therapeutic implementation of Iproniazid have been reduced [25]. In 1961 Iproniazid was withdrawn owing to the inadmissible ratio of hepatitis and was replaced by less hepatotoxic drugs such as isocarboxazid, phenelzine, and tranylcypromine [26].

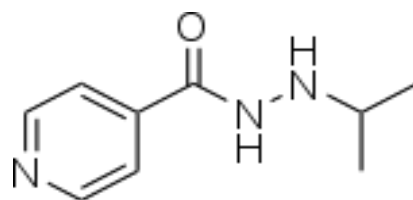


Figure 2.13. 2-D chemical structure of Iproniazid

Moclobemide was the first nonhydrazine, reversible MAO-A selective inhibitor approved for depression treatment. That was a potent inhibitor in vivo but

on the other hand it was a feeble inhibitor in vitro. It has been described as a 'slow binding inhibitor', whereby conformational changes to either Moclobemide or the enzyme to MAO-A slowly form a more tightly bound complex, resulting in the non-competitive MAO inhibition by Moclobemide [27]. Moclobemide is a benzamide derivative of morpholine ($O(CH_2CH_2)_2NH$) which acts pharmacologically as a selective, reversible inhibitor of MAO-A, a type of increases levels of especially serotonin, dopamine and norepinephrine [28].

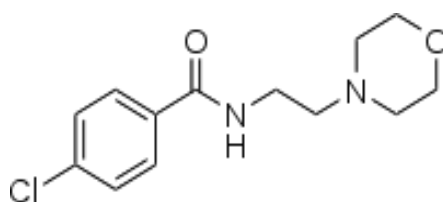


Figure 2.14. 2-D chemical structure of moclobemide

Chapter 3

3. Materials and Methods

3.1.1. General Properties of Molecular Docking

Docking is finding the binding geometry of two interacting molecules with known structures. Molecular docking is the crucial tool in computational biology and structure based drug design. After the determination of three-dimensional structure of proteins by X-ray crystallography and NMR importance of these 3-D structures has increased in last decade because of function of a protein depends primarily on its structure.

In the broadest sense, aim of the molecular docking is predicting molecular recognition and spatial conformation, to detection of potential binding positions withal optimal energy between two structures. Generally molecular docking is performed for a small molecule and a target macromolecule. Regard of the computer-aided drug design, molecular docking is computer simulation process to estimate of possible conformations of a binary complex that mostly between protein and ligand. Each docking software program uses own specific algorithms. Almost all docking software programs handle the rigid body protein, as an exception, Autodock 4.2. Software program allows side chains in the macromolecule to be flexible. Moreover molecular docking algorithms can be classified by two different forms. This classify is defined according to ligands structure selection such as flexible ligand or rigid body ligand.

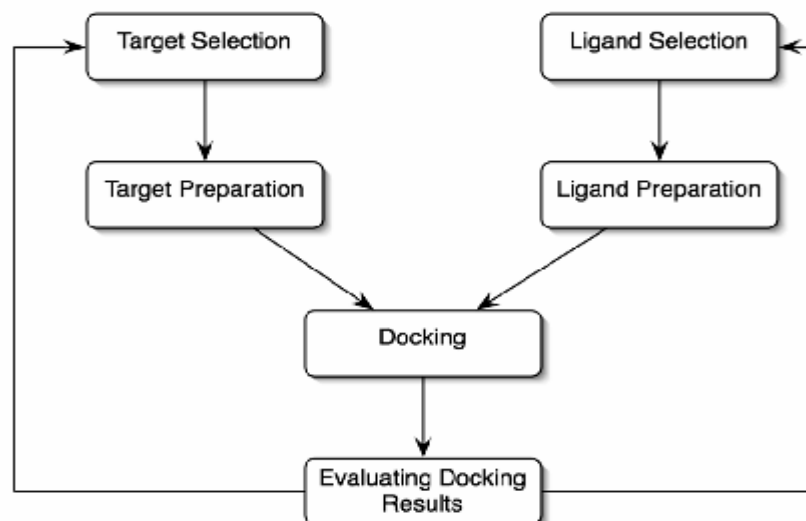


Figure 3.1. Workflow of docking studies

Rigid body docking algorithm is based on the geometric, volumetric, the atomic coordinates of the structure. Thus rigid body docking relates more the formal structure, but that causes some disadvantages as rigid body molecule cannot be a model for all molecules conformations. Owing to the fact that the computational costs increase exponentially with the degrees of freedom of molecules. As well as the rigid body ligand dockings occurs quickly than flexible ligand docking. Flexible docking algorithm is much harder than performing rigid-body docking. These flexible docking approaches consider free to rotate around its rotatable bounds of ligand molecule, that provides more accurate docking results of ligand and receptor cause of ligand is could alter of spatial conformations and that prevent such only one sample template for docking process. But disadvantage of this method causes too much computational costs and waste of the time.

The first step in docking studies is to identify regions on the protein structure that upon binding a ligand would interfere with normal function, such as an enzyme active site, the binding site of a receptor, or an allosteric site [29].

3.1.2. General Properties of AUTODOCK

Autodock (automated docking) is a most common docking software program and a major advantage is that open source. The main reason for arising Autodock is

bioactive compounds design and especially for computer aided drug design. It is conceived to estimate how small molecules, such as drug candidates, or substrates bind to a receptor of known three dimensional structure [30]. 3-D X-Ray crystallography structures that particularly proteins are stunning targets for understanding the principle biological activity and drug candidates. Herein, autodock is a crucial calculation tool for drug candidates because of measuring and predicting to molecular interactions and affinity.

Autodock offers a several of search algorithms to explore a given docking problem process. These search algorithms are Monte Carlo Simulated Annealing (SA), a Genetic Algorithm (GA) and a hybrid local search genetic algorithm which is known the Lamarckian Genetic Algorithm (LGA). Genetic algorithm is a search heuristic and mimics the natural evolution process. Genetic algorithms are inspired by natural evolution for generating solutions to optimization problems and that use similar methods such as mutation, crossover, selection and inheritance. These algorithms offer a set of solution instead only one solution. In a genetic algorithm a population of string which is also represent chromosomes or genotype of genome encode candidate solutions that includes creatures or phenotypes to an optimization problem and evolves toward better solutions.

Creators of Autodock are clearly specify that, the most efficient method is Lamarckian Genetic Algorithm that includes both of global search and local search methods.

Autodock 4.2 uses a semi empirical free energy force field for assessment of conformation in the course of docking simulation process. Force field could be consider in two parts for Autodock 4.2 model. Macromolecule or protein and the ligand launch in unbound conformation. Firtsly, the intramolecular energetics are estimated for the modulation from these unbound states to the conformation of the ligand and protein in the bound state, this is considerable for estimate of the conformational entropy lost upon binding. Secondly, intermolecular energetics of protein and the ligand combination is evaluated in their bound conformation. Force field includes six pairwise evaluations (V) and an estimate of the conformational entropy lost upon binding also includes the weighting constants (W) for optimize to calibre the empirical free energy in the binding equation that based on a several of

experimentally-determined binding constant and basis of molecular mechanics terms and entropic terms which are Van der Waals forces, Hydrogen Bonding, Coulombing potential, desolvation and torsional parameters are use these weighting constants. Free energy of binding equation represent as below equations.

$$\Delta G = (V_{bound}^{L-L} - V_{unbound}^{L-L}) + (V_{bound}^{P-P} - V_{unbound}^{P-P}) + (V_{bound}^{P-L} - V_{unbound}^{P-L} + \Delta S_{conf})$$

In this equation L represent ligand compound and P represent protein for proceses of protein-ligand docking.

$$V = W_{vdw} \sum_{i,j} \left(\frac{A_{ij}}{r_{ij}^{12}} - \frac{B_{ij}}{r_{ij}^6} \right) + W_{nbond} \sum_{i,j} E(t) \left(\frac{C_{ij}}{r_{ij}^{12}} - \frac{D_{ij}}{r_{ij}^{10}} \right) + W_{elec} \sum_{i,j} \frac{q_i q_j}{\epsilon(r_{ij}) r_{ij}} + W_{sol} \sum_{i,j} (S_i V_j + S_j V_i) e^{(-r_{ij}^2 / 2\sigma^2)}$$

For the purpose of calculation for free binding energy has a several process. The final intermolecular energy is calculated from total of van der Waals, hydrogen bond, desolvation, electrostatic energies and final internal energy, torsional energy of the ligand and the total energy of the unbound system.

3.1.3. General Properties of Accelrys Discovery Studio

Accelrys Discovery Studio is a software program that provides molecular design solutions for computational chemists and computational biologist especially in the areas of drug discovery and materials science. Accelrys Discovery Studio includes modern methods for docking. In this thesis Libdock is used by Accelrys Discovery Studio 3.1. During the docking process enzymes are handled as rigid and ligands are prepared flexibly so rotatable bonds are considered. [31]

Libdock based on work of David J. Diller [32]. Workflow of Libdock starts by conformational search such as Fast, Best, Caesar. Second step is hotspot generation that related protein aggregation. Next step is triplet match between hotspot and molecule which knowledge-based docking. The last step is final optimization.

Libdock provides four different conformation methods such as high quality, fast search, fast search for SASA (solvent accessible solvent area) and user specified but according to producers fast search is most appropriate for docking a very large

data set so in this study conformation method is setup fast search. Details of Libdock docking parameters are shown in Chapter 3.3.2

3.2. Preparing Compounds

3.2.1. Preparing Monoamine Oxidase Isozymes

Monoamine oxidase isozymes are classified in two forms which are monoamine oxidase A (MAO-A) and monoamine oxidase B (MAO-B). In this thesis known crystallized 3-D structures of both MAO isoenzymes are utilized from Protein Data Bank. (PDB) Crystal structure of Human Monoamine Oxidase A with Harmine [33] is used in this studies and experimental details of X-Ray diffraction in table 13.

Table 3.1

| Method | X- Ray Diffraction |
|-----------------------------|-----------------------|
| Resolution [\AA] | 2.20 |
| R-Value | 0.204 (obs.) |
| R-Free | 0.255 |
| Unitcell | |
| Length [\AA] | Angles [$^{\circ}$] |
| a = 135.26 | $\alpha = 90.00$ |
| b = 218.71 | $\beta = 90.00$ |
| c = 54.37 | $\gamma = 90.00$ |

Other known crystallized 3D structure of human Mao B in complex with safinamide [34] (2v5z) and two coumarin derivates all sharing a common bezylox substituent, were defined by X-RAY crystallography. Experimental details of X-Ray diffraction in table 14.

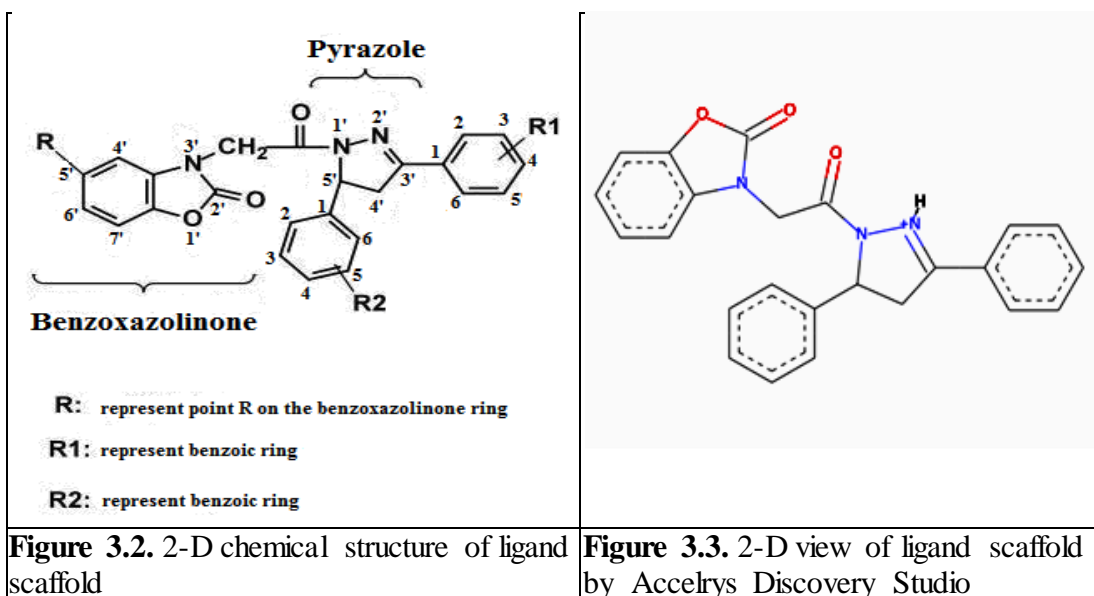
Table 3.2

| Method | X- Ray Diffraction |
|-----------------------------|---------------------|
| Resolution [\AA] | 1.60 |
| R-Value | 0.208 (obs.) |
| R-Free | 0.227 |
| Unitcell | |
| Length [\AA] | Angles [$^\circ$] |
| a = 132.55 | $\alpha = 90.00$ |
| b = 223.60 | $\beta = 90.00$ |
| c = 86.59 | $\gamma = 90.00$ |

Both of subtypes of Monoamine oxidase are obtained as the pdb format from protein data bank cause of the docking simulation studies are constituted for macromolecule based drug design.

3.2.2. Preparing Ligands of Monoamine Oxidase Isozymes

In this thesis, preparing of ligands are designed by based on the two different compound which are benzoxazolinone ring and pyrazole.



This scaffold is basis of the all ligands for MAO-A and MAO-B isozymes. On the other hand this scaffold was thought the lead compound for this thesis studies. Process of creating this scaffold is inspired by the preceding experimental and computational researches.

Table 3.4. Preparing code names of ligands.

| First code | Meaning of first code | Second code | Meaning of second code | Third code | Meaning of third code | Fourth code | Meaning of fourth code |
|------------|------------------------------|-------------|--|------------|--|-------------|------------------------|
| <i>1</i> | H added ring R | <i>a</i> | H added ring R1 | <i>1</i> | H added to R2 | <i>r</i> | -r stereo isomer |
| <i>2</i> | Cl added ring R | <i>b</i> | CH ₃ added 3. point of ring R1 | <i>2</i> | OCH ₃ added 2. point of ring R2 | <i>s</i> | -s stereo isomer |
| <i>3</i> | CH ₃ added ring R | <i>c</i> | OCH ₃ added 2. point of ring R1 | <i>3</i> | OCH ₃ added 3. point of ring R2 | | |
| | | <i>d</i> | OCH ₃ added 4. point of ring R1 | <i>4</i> | OCH ₃ added 4. point of ring R2 | | |
| | | <i>e</i> | CH ₃ added 5. point of ring R1 | <i>5</i> | OCH ₃ added 2. and 3. points of ring R2 | | |
| | | | | <i>6</i> | CH ₃ added 4. point of ring R2 | | |
| | | | | <i>7</i> | CH ₃ added 2. Point of ring R2 | | |

In the figure 3.2, ‘R’ represent fifth point of benzoxazolinone ring, ‘R1’ represent ring R1 and ‘R2’ represent ring R2.

Ligands name are generated by 4 part codes. These codes contain 2 special numbers and 2 special letters. Some ligands code names are such as 1a2r, 2c4s, 3e7r.

All ligands names start with a number that first part of code names are between 1 and 3.

Meaning of these codes;

1 → hydrogen (H) is added to R point of benzoxazolinone ring

2 → chloride (Cl) is added to R point of benzoxazolinone ring

3 → methyl (CH₃) is added to R point of benzoxazolinone ring.

For example, code '1' determinates that point R of scaffold has only hydrogen (H) atom. Code '2' determinates that point R of scaffold has only chloride (Cl) atom. Code '3' displays that point R of scaffold has only methyl (CH₃) compound.

Second code is related with another benzoike* ring that is indicated with R1. This second code is consist of letters as a, b, c, d and e. That letters display that spesific binding points and special compounds that are binding ring R1. Ring R1 has got 6 corners. Each corner of R1 has a number. These numbers are determinate for binding point of hydrogen (H), methoxy (OCH₃) and methyl (CH₃).

Meaning of these codes:

a → only hydrogen atoms are added to R1 ring

b → methyl (CH₃) is added to number 3 point of R1 ring.

c → methoxy (OCH₃) is added to number 2 point of R1 ring.

d → methoxy (OCH₃) is added to number 4 point of R1 ring.

e → methyl (CH₃) is added to number 5 point of R1 ring.

Third code is that has a number between 1 and 7, each number is related with binding points and adding compounds of ring R2. R2 ring has 6 corners as figure 3.2.

Meaning of third codes:

1 → only hydrogen element is added to ring R2

2 → methoxy (OCH₃) is attached to point number 2 of the ring R2

3 → methoxy (OCH₃) is attached to point number 3 of ring R2

4 → methoxy (OCH₃) is attached to 4.point of ring R2

5 → two methoxy (OCH₃) are attached to 2. point and 3. point of ring R2

6 → methyl (CH₃) is attached to 4.point of ring R2

7 → methyl (CH₃) is attached 2.point of ring R2.

Fourth and last code is consist of only two letters as ‘r and s’. These codes are related chiral center of ligands stereoisomerism. 105 ligands are created as –s stereoisomer and other 105 ligands are created as –r stereoisomer.

3.3. Molecular Docking

3.3.1. Docking Setup of AUTODOCK 4.2

AUTODOCK 4.2 requires 4 different input parameter files for properly running. These input files for each docking are, PDBQ file, GPF file and DPF file on the other hand AUTODOCK Tools (ADT) is a primary auxiliary for creating these files.

Macromolecule files are prepared by first adding polar hydrogen atoms.

Ligands are prepared by first nonpolar hydrogen atoms are merged and Gasteiger charges are added. Bonds with torsional freedom are marked obtained to PDBQ file.

Grid files constitute GPF files. During the producing GPF, points of grid size, grid center points, spacing between grid points and quantity of grid files which based on the atom types are defined as parameters. In this thesis two set of grid file is used. The first grid set is designed for MAO-A isozyme and second set is designed for MAO-B isozyme. Both of settings are designed for relatively fine docking. Map parameters are defined as 80x80x80 grid points for three dimension and spacing is kept default 0.375 Å. These parameters circle whole active side of the proteins. Grid center points of MAO-A isozyme are defined x: 33.625 y: 30.159 z: -18.303 on the xyz coordinate and grid center points of MAO-B isozyme are defined x: 53.506 y: 147.816 z: 24.376 on the xyz coordinate.

DPF contains docking algorithm and essential variable parameters for Autodock docking. Population size, number of energy evaluation, number of generation, number of runs, rate of crossover, rate of mutations are defined in

docking parameter file. In this thesis these parameters are improved from default units for fine docking. Population size: 150, number of energy evaluation: 5000000, number of generation 27000, number of run: 50-100, crossover rate: 0.8, mutation rate: 0.02.

3.3.2 Enzyme-Ligand Molecule Docking by AUTODOCK 4.2

In this thesis Autodock is performed for MAO-A and MAO-B isozymes. For each isozymes of MAO is prepared in the AUTODOCK 4.2 using the parameter set up.

MAO A and MAO B enzymes were handled separately in this software program. Firstly MAO A enzyme is docked with 210 many ligands specially half of these ligands have r stereoisomerism and other half of these ligands have s stereoisomerism. Goal of the using that two different stereoisomerism is detecting of the best prediction lowest energy value during the docking of ligand and enzyme. This stereoisomerism is generated for all ligands thus all ligands are obtained in pairs.

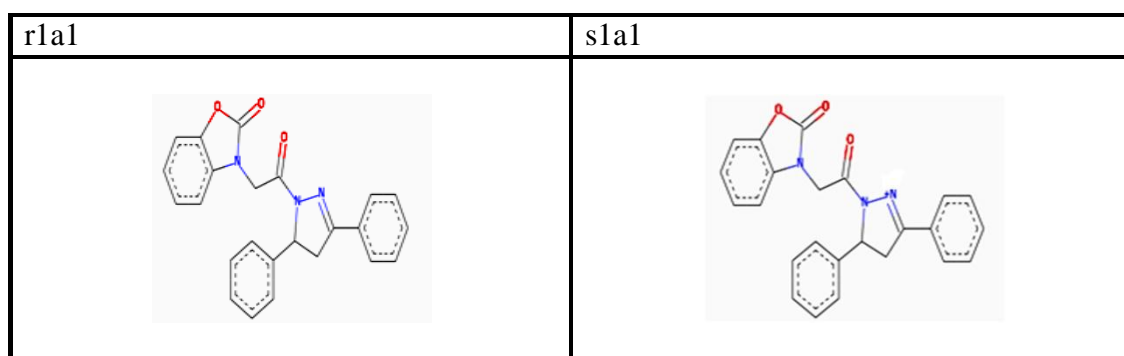


Figure 3.4. Comparing –r and –s stereoisomers of ligands by Accelrys Discovery Studio

MAO A enzyme is performed respectively 105-r stereoisomer ligands and 105-s stereoisomer ligands by the using docking set up parameters as mentioned in chapter 3.3.1. Docking results are in the supplementary.

MAO-B enzyme is performed with the same ligands as MAO-A docking process. 105-r stereoisomer ligands and 105 s isomer ligands are docked one by one with MAO B isozyme. Docking set up parameters created as mentioned in chapter

3.3.1. The only difference between MAO A is grid box parameters cause of active side of MAO isozymes have different coordinates.

3.3.3 Docking Setup of LIBDOCK

Accelrys Discovery Studio 3.1 requires two main input parameters for properly docking process. These parameters are enzyme file and ligand file. Enzyme file format is converted to dsv format from format pdb for each MAO-A and MAO-B by Accelrys likewise ligand file is converted to sd format from format pdb by Accelrys. During prepare of ligands, according to results of Autodock the best 10 ligands for MAO-A and the best 10 ligands for MAO-B are prepared for Libdock process.

Firstly enzyme and ligand parameters are inserted to Accelrys, secondly enzyme and ligand are defined. Before the defined of enzyme cavity, hydrogen atoms are added for the best work of cavity method. Before the docking process, special parameters of Libdock are defined. In the course of MAO-A Libdock perform, input enzyme sapphire xyz coordinates are defined as x: 25.717, y: 37.50, z: -15.287 and radius: 14.169 other parameters set up as number of hotspots: 100, docking tolerance: 0.25, docking preferences: high quality, conformation method: fast, minimized algorithm: do not minimize. On the other side, MAO-B enzyme sapphire xyz coordinates defined as x: 46.238, y: 162.147, z: 36.200 and radius: 19.60 other parameters set up as number of number of hotspots: 100, docking tolerance: 0.25, docking preferences: high quality, conformation method: fast, minimized algorithm: do not minimize.

After the docking process, results are ranked in order to libdock score in output file.

Chapter 4

4. Result and Discussion

4.1. Results of Molecular Docking Studies by Autodock 4.2

The data set of 210 ligand compounds described in Chapter 3 are docked to monoamine oxidase A isozyme by running AUTODOCK 4.2 software program that is calculated results using the Lamarckian genetic algorithm.

The best ligand molecules and their scoring functions are categorized which are top ten ranked in classify of r and s stereoisomerism used to rank them are listed in table 4.1. These molecules are chosen from 210 different ligands and classified for drug candidates for MAO-A and MAO-B isozymes.

Docking studies by MAO-A show that ligands of first code name include '1' have high score than other ligands such as code names starting with '2' and '3'. Thus, when only hydrogen is attached R point of scaffold bind to MAO-A enzyme more effective than other ligands which have chloride and methyl on R point of benzoxazolinone. The best docking result for MAO-A is obtained by ligand 1d3r. Free binding energy of 1d3r is -13.09 kcal/mol and estimated inhibition constant is 252.50 pM. This result indicates at the lowest docking energy conformation, methoxy that is on 3 position of ring R1 makes hydrogen bonding by Lys305 and methoxy which is on the 4 position of ring R2 makes another hydrogen bonding by Tyr197. Second good docking result is obtained by 1d6r docking that has -12.77 kcal/mol free binding energy and estimated inhibition constant is 435.24 pM. Other high score ligands after the Autodock studies are ordinarily 1a3r, 1d1r, 1a6r, 1c3r, 1c6r, 3e6r, 2c7s and 1d7s. Detailed result values are in the table Y.

Considerable that r-stereoisomerism much effective than s-stereoisomerism for MAO-A isozyme. According to results, only two s-isomers such as 2c7s and 1d7s are observed in the top ten results of docking MAO-A studies.

On the other hand, MAO-B docking results show that ligand 2d1r consist the best docking with MAO-B. Free binding energy is -13.35 kcal/mol and estimated inhibition constant is 165.01 pM. Methoxy (OCH₃) on the ring R1 makes sigma - π interaction with FAD. Also Tyr435 and FAD make sigma - π interactions with ring R1, Tyr188 and Tyr398 makes π - π interactions with ring R1. Second good docking result is obtained by 1d4s. Free binding energy is -11.69 kcal/mol and estimated binding constant is 2.69 nM. Hydrogen atom that determinate s-stereo isomer makes close interaction with Tyr 326. Other good docking results are obtained by ligands 1d5s, 1d6s, 1d3s, 1a3s, 1a1s, 3b4r, 1c6s and 3d4s.

According to these results, s-stereo isomers give high scores for docking MAO-B isozyme on the contrary MAO-A isozyme. Although the best result is an r-isomer (2d1r), eight docking results are obtained by s-isomers in the best 10 results for MAO-B docking.

On the other hand, according to docking results estimated inhibition constants (Ki) of MAO-A docking are better than MAO-B docking results.

Table: 4.1. Top 20 Autodock docking results of MAO-A and MAO-B isozymes

| MAO-A | | MAO-B | |
|---------|--|------------------------------------|---------|
| Ligands | Average binding free energy (kcal/mol) | Estimated Inhibition Constant (Ki) | Ligands |
| 1d3r | -13.09 | 252.50 pM | 2d1r |
| 1d6r | -12.77 | 435.24 pM | 1d4s |
| 1a3r | -12.63 | 50.71 pM | 1d5s |
| 1d1r | -12.61 | 570.20 pM | 1d6s |
| 1a6r | -12.59 | 589.50 pM | 1d3s |
| 1c3r | -12.56 | 621.24 pM | 1a3s |
| 1c6r | -12.53 | 654.87 pM | 1a1s |
| 3e6r | -12.38 | 848.42 pM | 3b4r |
| 2c7s | -12.24 | 1.16 nM | 1c6s |
| 1d7s | -12.09 | 1.38 nM | 3d4s |

4.2. Results of Molecular Docking Studies by LIBDOCK

After the Autodock 4.2 studies the best docking results are analyzed by Libdock tool of Accelrys Discovery Studio 3.1. These results include 20 ligands for MAO-A and MAO-B. These ligands are prepared for the Libdock as chapter 3.3.2.

...

Libdock docking based on poses of ligand and enzyme. Each docking process come true by these poses. Every one of ligands makes their specific conformation at the active side of enzyme. Thus produced poses are key role for the docking. MAO-A docking studies shows that less poses produced and as a result scores of ligands could not effective for MAO-A ligands. In respect of Libdock, score of ligand 1a3r is 114.80 and score of ligand 1a6r is 101.46 thus these ligands are better candidates for MAO-A inhibitor.

On the other hand, MAO-B docking process produced a greater number poses than MAO-A docking process, thus scores of MAO-B docking are observed much more effective. Specially ligand 2d1r, 1d6s, 3b4r, 1a1s, 1d3s are strong candidate. Score of ligand 2d1r is 141.08, score of ligand 1d6s is 145.86, score of ligand 3b4r is 143.824, score of ligand 1a1s is 143.66 and score of ligand 1d3s is 138.28. These results indicate that ligands are much effective for MAO-B than MAO-A. Detailed libdock scores of both MAO-A and MAO-B are given in the table x.

Table 4.2. Results of Libdock docking for MAO-A and MAO-B isozymes

| MAO-A | | MAO-B | |
|---------|---------------|---------|---------------|
| Ligands | Libdock Score | Ligands | Libdock Score |
| 1d3r | 90.79 | 2d1r | 141.08 |
| 1d6r | 91.85 | 1d4s | 97.16 |
| 1a3r | 114.80 | 1d5s | 92.16 |
| 1d1r | 95.70 | 1d6s | 145.86 |
| 1a6r | 101.46 | 1d3s | 138.28 |
| 1c3r | 98.75 | 1a3s | 125.50 |
| 1c6r | 94.16 | 1a1s | 143.66 |
| 3e6r | 105.318 | 3b4r | 143.824 |
| 2c7s | 92.16 | 1c6s | 112.02 |
| 1d7s | 87.24 | 3d4s | 111.30 |

4.3. Analysis of Monoamine Oxidase A – Ligand Docking

Ligand 1d3r

Pyrazole, benzoxazolinone and R2 parts of ligand 1d3r are positioned vertical towards FAD and R1 ring of ligand is positioned horizontal. Also inhibitor is surrounded by hydrophobic Leu337, Phe352, Tyr407 and Tyr197 residues at the lowest energy conformation moreover Ile335, Ile180, Asn181, Ile207, Asp338, Phe208 other residues that surround ligand 1d3r. In addition residues Tyr69, Ala68 and Gly67 are located close to FAD.

Tyr407 makes hydrogen bond (1.8\AA) with the oxygen atom of benzoxazolinone ring and shows π - π interaction (3.6\AA) by R1. Another π - π interaction (4.4\AA) occurs between Phe352 and benzoxazolinone. Tyr197 located close to aromatic cage and positioned horizontally to R2 make one hydrogen bond (2.4\AA) by the oxygen atom of methoxy on the ring R2. Other hydrogen bonds are observed between the Lys305 and oxygen atom of methoxy on the ring R1. Distances of these hydrogen bonds are 2.3\AA and 2.6\AA .

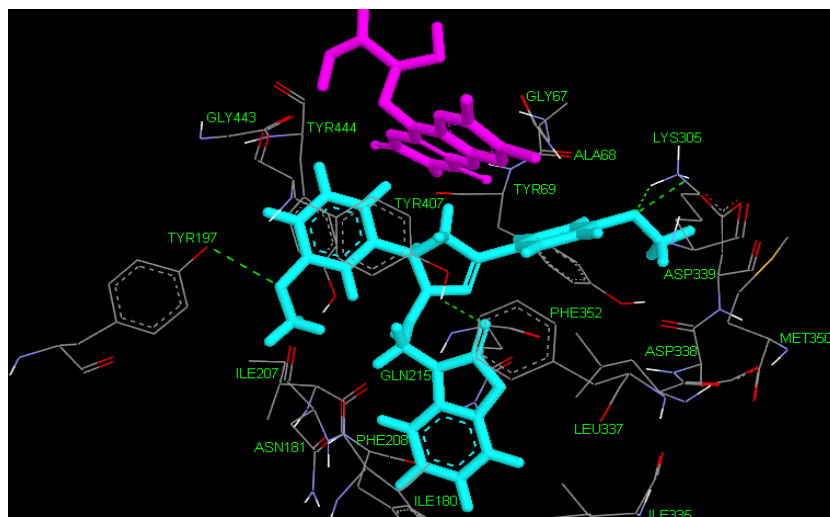


Figure 4.1. 3-D view of ligand 1d3r and active side of MAO-A at the lowest energy conformation. Pink color represent FAD compound, cyan color represent inhibitor, green dashed line represent hydrogen bonding.

Ligand 1d6r

Ligand 1d6r has hydrogen at the R point, methoxy at the fourth point of ring R1, methyl at the fourth point of ring R2. Benzoxazolinone ring get involved among of two amino acid side chains range where are Tyr444, Gln215, Ile180 and Tyr407, Leu337, Phe352, Tyr69. Especially residues Tyr444 and Tyr407 are located so close to aromatic cage. Other residues of surrounding ligand are Tyr197, Ile207, Phe208, Met 350, Ile335 and hydrophilic Asp338 at the lowest energy conformation of docking MAO-A isozyme.

There is 2 hydrogen bounds are obtained. First one occurs between Tyr407 and oxygen of benzoxazolinone (1.9 Å). Second hydrogen bond is observed between Lys305 and oxygen of methoxy group of R1 ring. Otherwise FAD does a sigma - π interaction with R2 ring (2.4 Å). Tyr 407 makes π - π interactions with ring R2 (3.3 Å), Tyr444 makes another π - π interactions with benzoxazolinone.

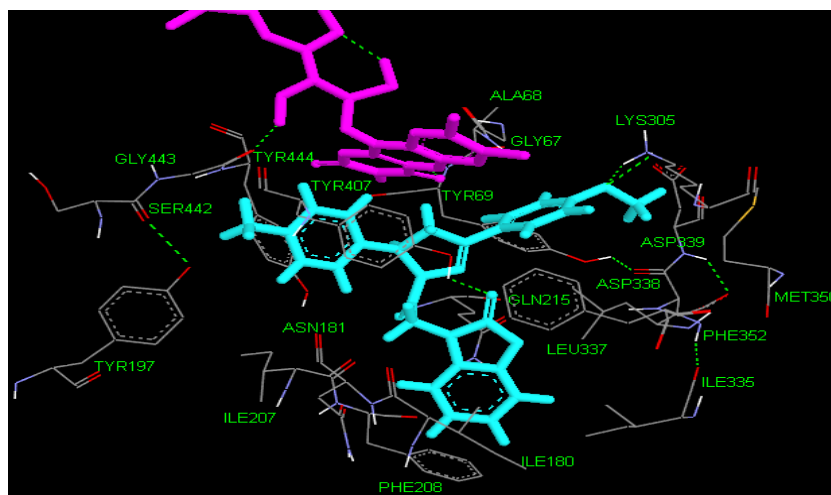


Figure 4.2. 3-D view of ligand 1d6r and active side of MAO-A at the lowest energy conformation. Pink color represent FAD compound, cyan color represent inhibitor, green dashed line represent hydrogen bonding.

Ligand 1a3r

Chemical structure of ligand 1a3r that scaffold has hydrogen at the point R, only hydrogen atoms are at the ring R1 and methoxy is at the third point of ring R2. Ligand 1a3r is located to the active side of MAO-A by a good clean geometry. Benzoxazolinone ring of the ligand is located to between two hydrophobic pockets that are Tyr407, Phe352, Leu337 and Ile335, Gln215, Tyr444. Pyrazole is positioned

between the Tyr69, Lys218 amino acid side chains and FAD. Also Ile207, Asn181, Ile207 and Met350 are other residues which surrounding of the ligand.

FAD and Ring R2 have sigma – π interaction (2.4 Å). Oxygen of benzoxazolinone ring makes hydrogen bound by hydrophobic Tyr407 (2.2 Å). Also Tyr407 does π - π interaction with the ring R1 (3.4 Å). Other π - π interaction is obtained between the Phe352 and benzoxazolinone ring (4.4 Å).

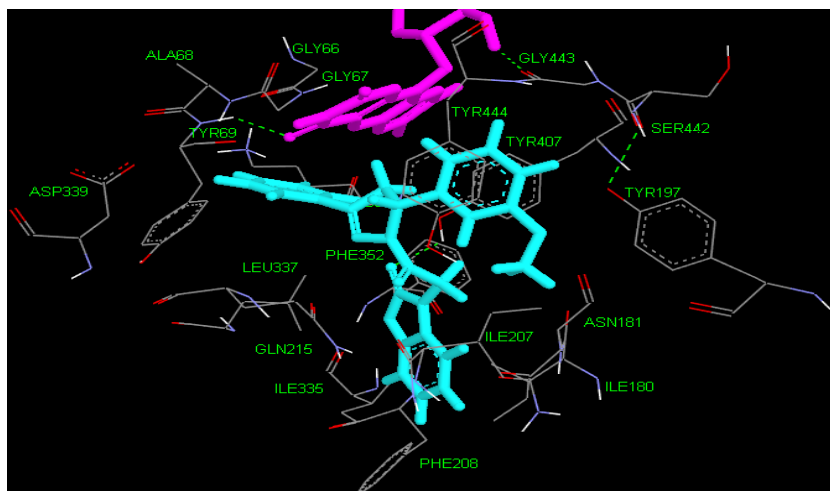


Figure 4.3. 3-D view of ligand 1a3r and active side of MAO-A at the lowest energy conformation. Pink color represent FAD compound, cyan color represent inhibitor, green dashed line represent hydrogen bonding.

Ligand 1d1r

Benzoxazolinone, pyrazole and ring R2 positioned horizontally to each other and positioned vertically to ring R1 and FAD at the active side of MAO-A isozyme. Ligand conformation is located between amino acid side chains of hydrophobic Tyr444, Ile180, Ile207 and Leu337, Phe352, Tyr407 thence makes close contact with FAD. Also hydrophilic Asp339, Lys305, Lys218, Asp64 residues surround ring R1 within 4.5 Å at the lowest energy conformations.

Tyr407 makes a hydrogen bond of good geometry with the oxygen of benzoxazolinone (2.0 Å). Another hydrogen bond that length is 2.4 Å occurs between oxygen of ring R1 and hydrophilic Lys305. π – π interaction consist of Tyr407 and ring R2 (3.5 Å). Another π – π interaction that distance is 4.3 Å occurs between the oxygen of benzoxazolinone ring and residue Leu337.

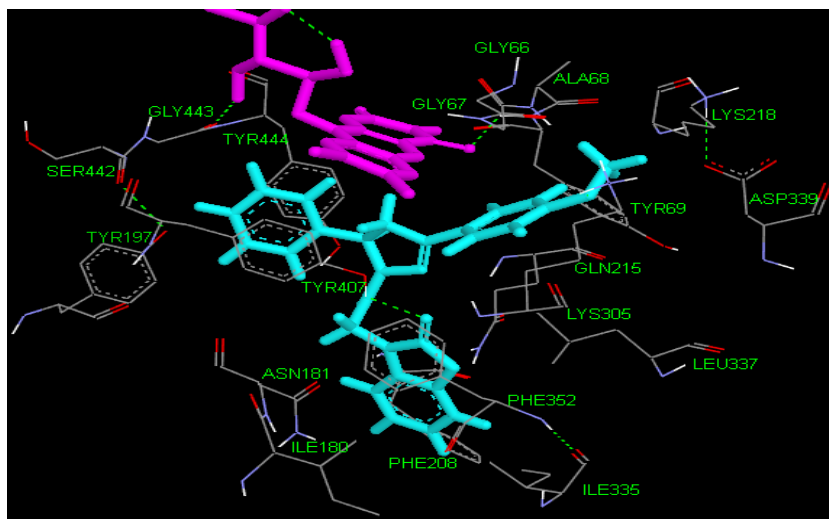


Figure 4.4 3-D view of ligand 1d1r and active side of MAO-A at the lowest energy conformation. Pink color represent FAD compound, cyan color represent inhibitor, green dashed line represent hydrogen bonding.

Ligand 1a6r

Conformation of ligand 1a6r is similar with ligand 1d3r at the lowest energy conformation of docking MAO-A. Aromatic cage is surrounded by Tyr407, Tyr444, Gln215, Ile180 and Leu337 residues. Also residues Phe208, Asn181, Gln215, Phe352 are close to benzoxazolinone ring. Other residues that surround of ligand 1a6r are Ala68, Gly67, Lys305, Tyr197.

Residue Tyr407 and oxygen atom of benzoxazolinone makes hydrogen bonding (2.1Å) and same residue where located to aromatic cage generates π - π interaction (3.3Å) with ring R2. Hydrophobic Phe352 makes π - π interaction (4.4Å) with benzoxazolinone. In addition significant sigma- π interaction (2.3Å) occurs between FAD and ring R2.

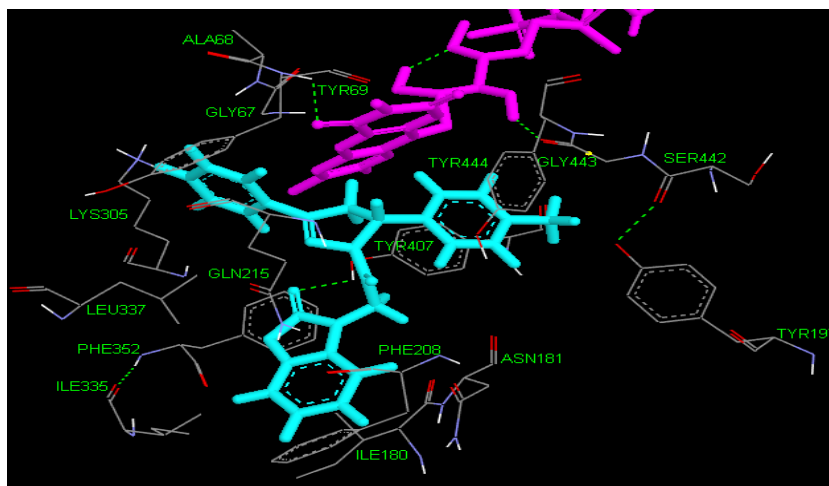


Figure 4.5. 3-D view of ligand 1a6r and active side of MAO-A at the lowest energy conformation. Pink color represent FAD compound, cyan color represent inhibitor, green dashed line represent hydrogen bonding.

Ligand 1c3r

Conformation of inhibitor 1c3r is located quite close to FAD. Aromatic cage is clearly shown with a good geometry. When ring R2 and benzoxazolinone are positioned horizontally for each other FAD and ring R1 are positioned vertically at the lowest energy conformation. Analysis of 3D structure of inhibitor position shows that aromatic cage remains among to hydrophobic residues Tyr407, Leu337, Phe352 and Tyr444. Also residues such as Tyr197, Tyr444, Lys305, Leu317, Ile180, Phe208 and Ile207 surround ligand 1c3r.

Important residue Tyr407 is associated with oxygen atom of benzoxazolinone by hydrogen bond (2.2\AA) and this residue makes π - π interaction (3.4\AA) with ring R2. Hydrophobic residue Phe352 makes another π - π interaction (4.4\AA) by five carbon ring of benzoxazolinone.

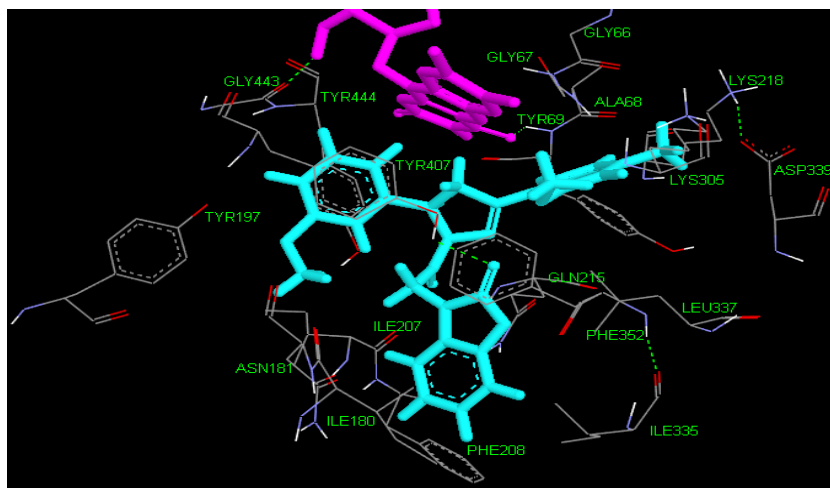


Figure 4.6. 3-D view of ligand 1c3r and active side of MAO-A at the lowest energy conformation. Pink color represent FAD compound, cyan color represent inhibitor, green dashed line represent hydrogen bonding.

Ligand 1c6r

This inhibitor shows high degree similarity with inhibitor 1c3r about position at the lowest energy conformation. Residues Tyr407, Tyr69 and Tyr444 are located close to aromatic cage. Other considerable residues Leu337, Tyr197, Ser442, Gln215, Ile180 and Lys305 surround ligand 1c6r.

In the ligand 1c6r docking process small number interactions are obtained. Tyr407 and benzoxazolinone has hydrogen bond (2.4Å) and Tyr407 makes π - π interaction with R2 (3.0Å). Other π - π interaction occurs between Phe352 and benzoxazolinone.

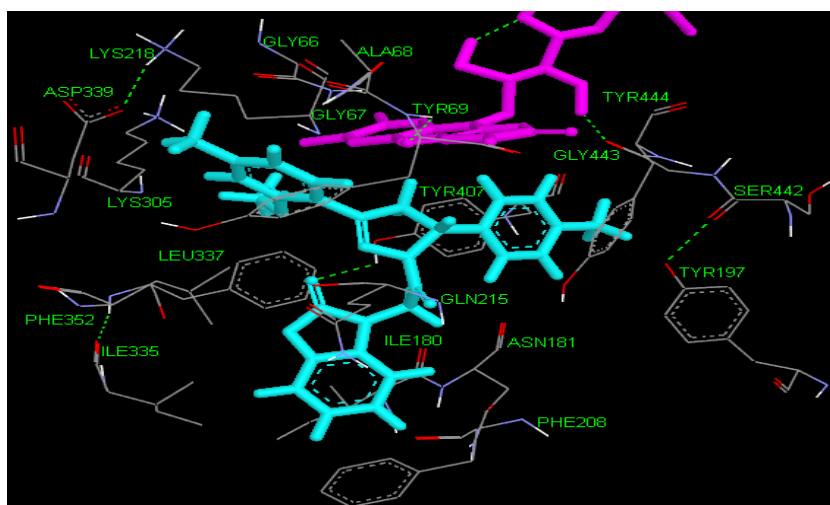


Figure 4.7 3-D view of ligand 1c6r and active side of MAO-A at the lowest energy conformation. Pink color represent FAD compound, cyan color represent inhibitor, green dashed line represent hydrogen bonding.

Ligand 3e6r

Hydrophobic residues Tyr407, Phe352, Leu337 are located close to aromatic cage. When Ile207 and Ile180 positioned near to benzoxazolinone, residues Tyr444, Gln215, Tyr197 are positioned around ring R2. Other residues Gly443, Ser442, Tyr69, Lys305 and Asn181 surround the ligand 3e6r.

In this docking analysis, three interactions are obtained. Residue Tyr407 and ring R2 makes π - π interaction (3.4Å). Tyr444 and benzoxazolinone ring does hydrogen bonding (1.7Å). Last interaction for ligand 3e6r is sigma- π that occurs between the benzoxazolinone and ring R2.

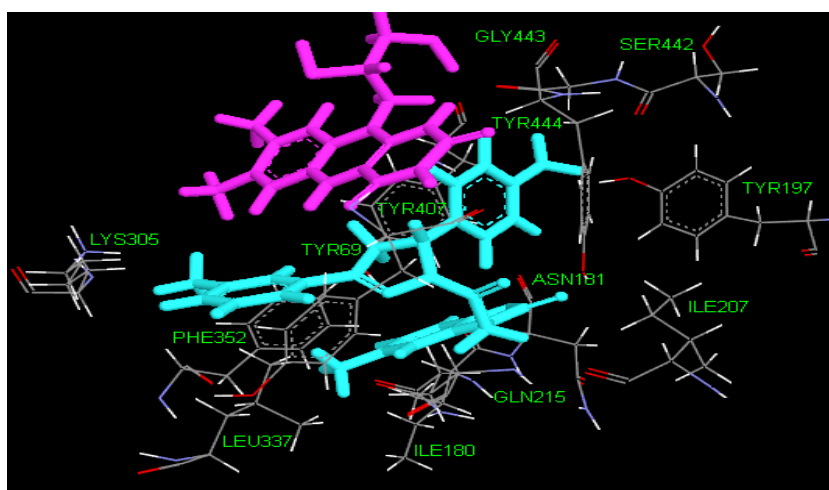


Figure 4.8. 3-D view of ligand 3e6r and active side of MAO-A at the lowest energy conformation. Pink color represent FAD compound, cyan color represent inhibitor, green dashed line represent hydrogen bonding.

Ligand 2c7s

Residue Tyr444 is located almost central of aromatic cage. Benzoxazolinone ring is positioned between residues Ile335, Asn181, Ile180, Tyr197 and hydrophobic pocket residues such as Tyr407, Ile207, Leu337. Other residues Tyr69, Ala68, Gly67, Phe208, Phe352 and Val182 surround ligand.

Tyr407 has important role for 2c7s docking results. Ring R2 and Tyr407 makes cation- π interaction (4.2Å). Also hydrogen bonding occurs between the Tyr407 and benzoxazolinone (2.1 Å). Another interaction is observed as π - π (5.5Å). This interaction occurs between the Tyr444 and ring R1.

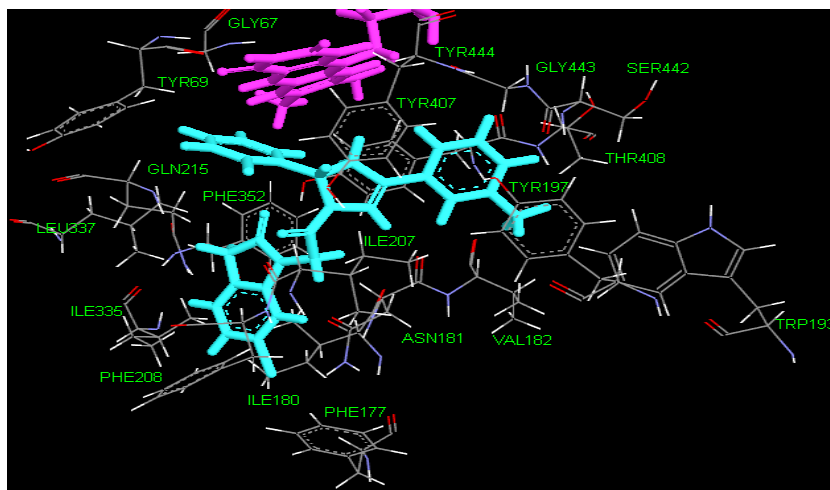


Figure 4.9. 3-D view of ligand 2c7s and active side of MAO-A at the lowest energy conformation. Pink color represent FAD compound, cyan color represent inhibitor, green dashed line represent hydrogen bonding.

Ligand 1d7s

Residues Leu337, Gly67, Gln215 are positioned at the aromatic cage. Pyrazole is located between the hydrophobic packet residues Ile335, Phe177, Ile180, Phe208 and other hydrophobic residues Tyr407 and Phe352. Also Tyr444, Tyr197, Ala68, Tyr69 and Gly443 are other residues that surround the ligand 1d7s.

Benzoxasazolinone and Lys305 make cation- π interaction (4.0 Å). Another cation- π interaction occurs between the Phe352 and nitrogen atom of pyrazole (5.4 Å) and also Phe352 makes π - π interaction with ring R1 (5.6 Å). Other π - π interaction occurs between the Tyr407 and ring R2 (3.3 Å). On the other hand, FAD makes a cation- π interaction with nitrogen atom of pyrazole (6.0 Å). Moreover FAD makes hydrogen bonding with oxygen atom of benzoxazolinone.

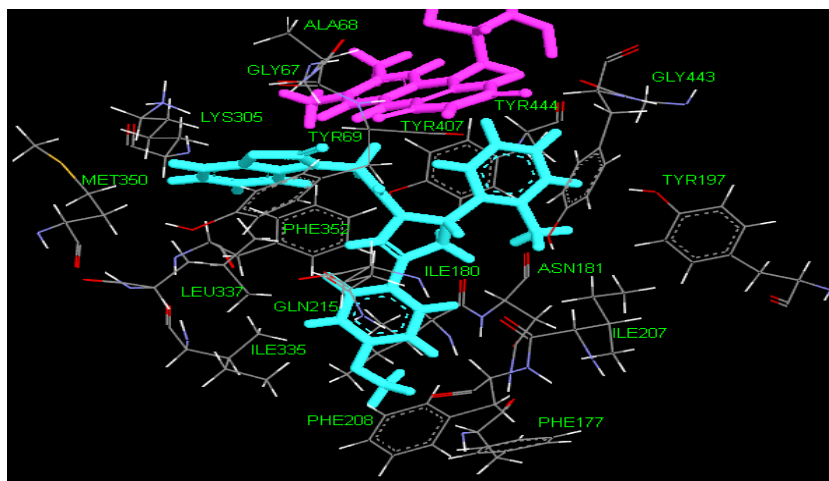


Figure 4.10. 3-D view of ligand 1d7s and active side of MAO-A at the lowest energy conformation. Pink color represent FAD compound, cyan color represent inhibitor, green dashed line represent hydrogen bonding.

4.4. Analyses of Monoamine Oxidase B - Ligand Docking

Ligand 2d1r

Ligand 2d1r is located active side of MAO-B isozyme and ring R1 of ligand is surrounded by hydrophobic pockets such as Tyr435, Tyr188 Tyr398. Also ligand has close interaction by FAD. Oxygen of pyrazole makes hydrogen bonding with Gln206 (2.3 Å). Besides hydrogen bonding very significant interactions are watched around the ring R1. $\pi - \pi$ interaction is shown between Try435 and R1 ring (3.9 Å). Also FAD performs 2 many sigma - π interactions. (2.9 Å, 2.6 Å)

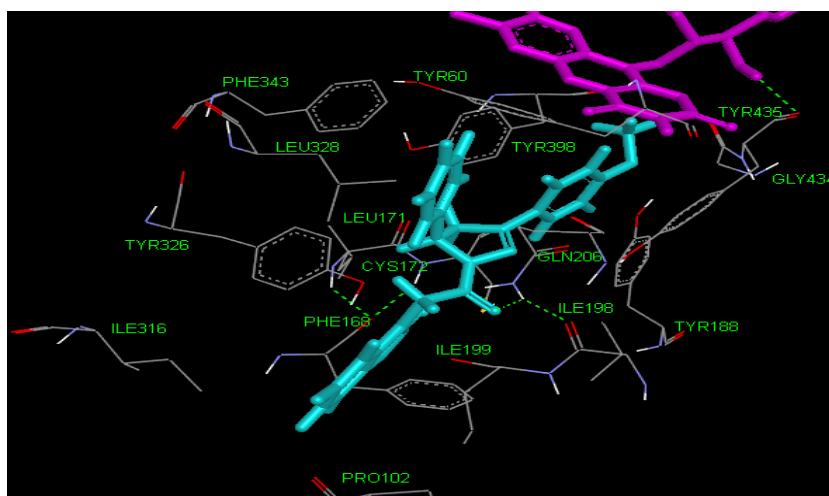


Figure 4.11. 3-D view of ligand 2d1r and active side of MAO-A at the lowest energy conformation. Pink color represent FAD compound, cyan color represent inhibitor, green dashed line represent hydrogen bonding.

Ligand 1d4s

Benzoxazolinone of ligand 1d4s is surrounded by hydrophobic Tyr435, Tyr398, Leu171 Ile199 amino acid side chains. Also benzoxazolinone is positioned near to FAD. Other hydrophobic amino acid side chains Cys172, Ile198, and Leu171 are positioned close to pyrazole. In addition Gly57, Met436, Lys296, Ser59, Tyr60, Phe433 amino acid side chains and Gly434, Thr399 Phe168, Phe103 amino acid side chains enclose the ligand.

Nitrogen of pyrazole makes hydrogen bound with non amino acid, the same nitrogen performs cation - π interaction by hydrophobic Tyr326 residue (5.9 Å). On the other hand other interactions occur around the benzoxazolinone ring. Tyr435 makes two different $\pi - \pi$ interactions with the benzoxazolinone ring (3.6 Å, 3.7 Å). Moreover Tyr 188 does another $\pi - \pi$ interaction with benzoxazolinone ring (5.9 Å).

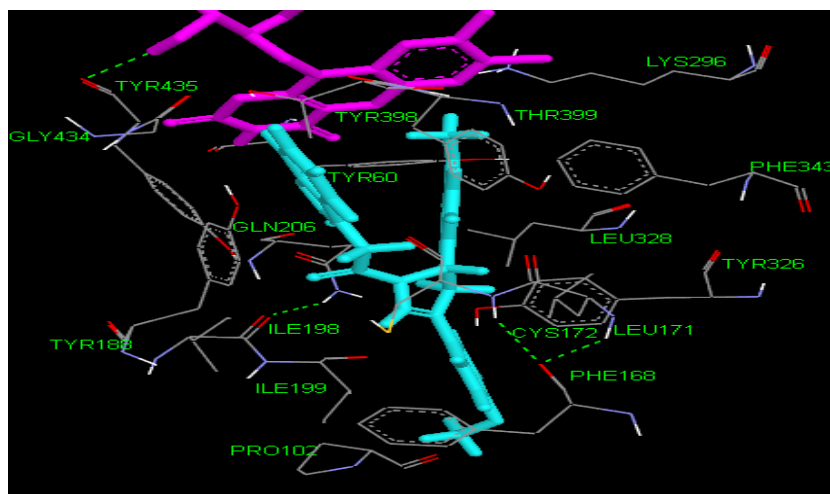


Figure 4.12. 3-D view of ligand 1d4s and active side of MAO-A at the lowest energy conformation. Pink color represent FAD compound, cyan color represent inhibitor, green dashed line represent hydrogen bonding.

Ligand 1d5s

Ligand 1d5s is located to the active side of MAO-B isozyme. FAD is shown near to benzoxazolinone ring of ligand. Pyrazole is surrounded by Cys172, Ile198, hydrophobic Tyr326, Leu171 and Gln206 amino acid side chains. In addition Ile199 is located near to ring R1 and Phe343, Tyr60 amino acid side chains are positioned close to ring R2. Nitrogen of pyrazole makes hydrogen bonding with non-aminoacid and has cation - π interaction by Tyr326 (5.9 Å). Benzoxazolinone ring occurs two

many $\pi - \pi$ interactions by hydrophobic Tyr435. (3.6 Å, 3.7 Å). Also benzoxazolinone ring makes another $\pi - \pi$ interaction with Tyr188 (5.9 Å).

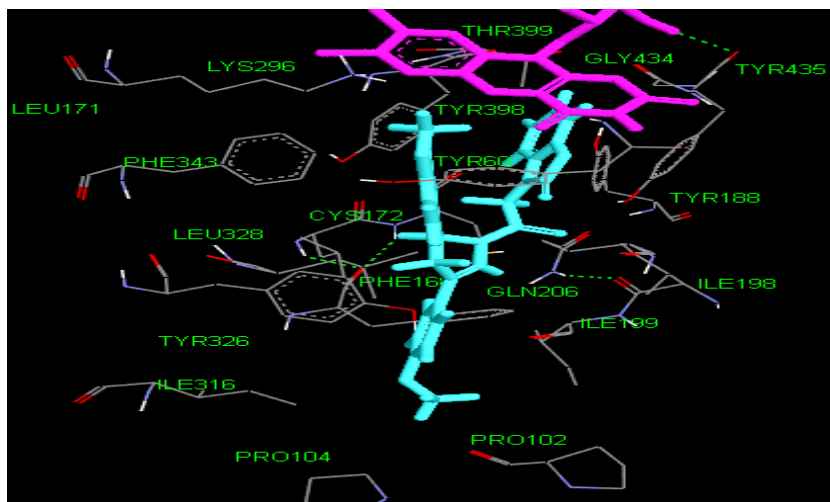


Figure 4.13. 3-D view of ligand 1d5s and active side of MAO-A at the lowest energy conformation. Pink color represent FAD compound, cyan color represent inhibitor, green dashed line represent hydrogen bonding.

Ligand 1d6s

Benzoxazolinone and R2 of inhibitor contact close to FAD. Tyr398, Tyr435, Tyr326, Cys172, Gln206 and Leu171 residues are located close to aromatic cage. Major hydrophobic residue Tyr435 creates two $\pi - \pi$ interactions with benzoxasazolinone (3.7Å – 5.6Å). Another $\pi - \pi$ interaction (5.8Å) is observed between the Tyr188 and benzoxasazolinone. Tyr326 and nitrogen of pyrazole show cation- π interaction (5.9 Å).

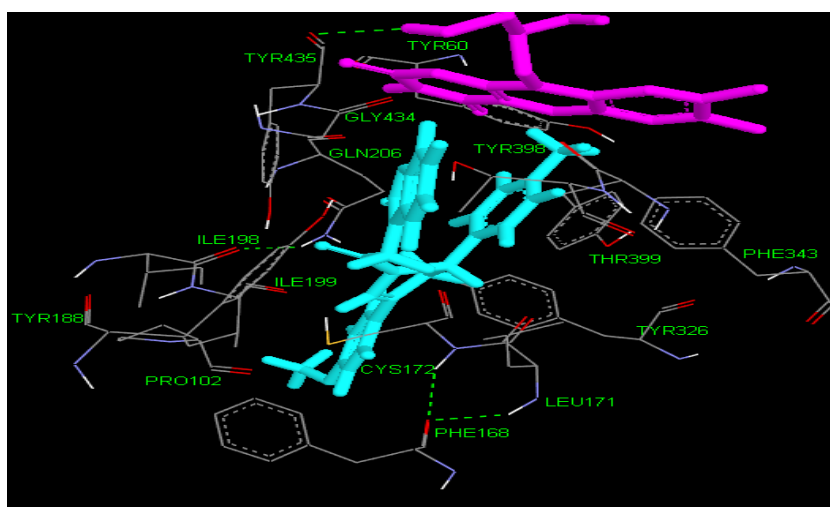


Figure 4.14. 3-D view of ligand 1d6s and active side of MAO-A at the lowest energy conformation. Pink color represent FAD compound, cyan color represent inhibitor, green dashed line represent hydrogen bonding.

Ligand 1d3s

Tyr435, Leu171 and Ile199 consist a hydrophobic packet close to aromatic cage. On the other hand Tyr398, Tyr326 and Phe343 residues enclose inhibitor.

Active role residue Tyr435 makes two π - π interactions with benzoxazolinone ($3.6\text{\AA} - 3.7\text{\AA}$). Another important residue Tyr326 and hydrogen atom of pyrazole generate a sigma- π interaction. Also a cation- π (5.9\AA) interaction occurs between the Tyr326 and nitrogen atom of pyrazole.

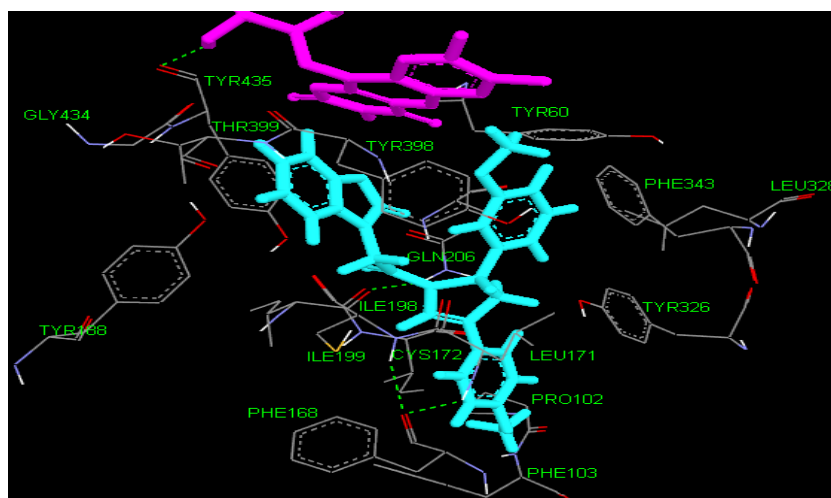


Figure 4.15. 3-D view of ligand 1d3s and active side of MAO-A at the lowest energy conformation. Pink color represent FAD compound, cyan color represent inhibitor, green dashed line represent hydrogen bonding.

Ligand 1a3s

Benzoxazolinone and Tyr435 occur two π - π interactions ($3.6\text{\AA} - 3.7\text{\AA}$). Tyr398 where located close to aromatic cage makes π - π interaction (6\AA) with R2. Nitrogen of pyrazole and Tyr326 make a cation- π interaction (5.9\AA). Also Gln206, Tyr188, Ile198, Ile199 and Phe342 are other residues where surrounding inhibitor.

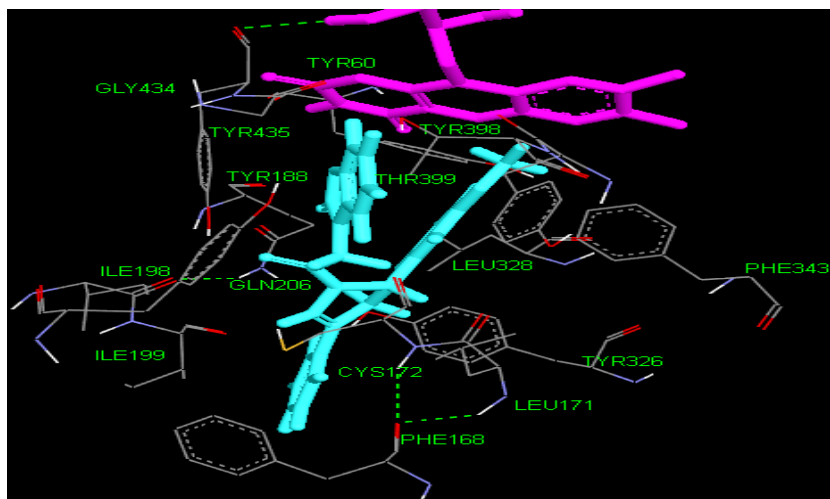


Figure 4.16. 3-D view of ligand 1a3s and active side of MAO-A at the lowest energy conformation. Pink color represent FAD compound, cyan color represent inhibitor, green dashed line represent hydrogen bonding.

Ligand 1a1s

Tyr326 and nitrogen of pyrazole consist in a cation- π interaction (5.9 Å). Tyr435 makes two π - π interactions with benzoxazolinone ring (3.6Å – 3.7Å). Another π - π interaction occurs between Tyr188 and benzoxazolinone ring. Also hydrophobic pocket that is formed by Ile198, Ile199, Phe343 and Gln206, Leu171 enclose the inhibitor.

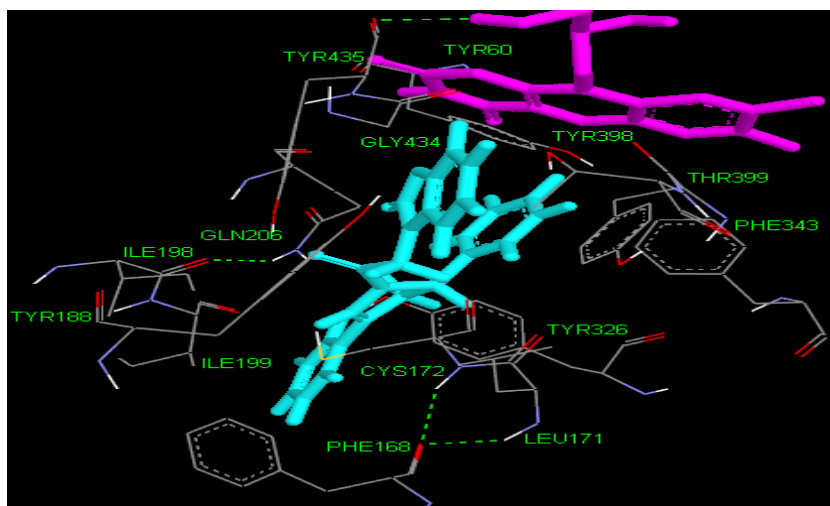


Figure 4.17. 3-D view of ligand 1a1s and active side of MAO-A at the lowest energy conformation. Pink color represent FAD compound, cyan color represent inhibitor, green dashed line represent hydrogen bonding.

Ligand 3b4r

Ligand 3b4r is conformed close to FAD of MAO-B isozyme. Specially ring R2 is located near the FAD. Pyrazole of ligand is positioned close to LEU171 and benzoxazolinone ring is located between Ile198, Tyr326 and Gln206, Leu171 residues.

Two critical interactions are obtained at the active side of MAO-B. Oxygen of pyrazole does hydrogen bonding by Cys172 (2.5 Å) and $\pi - \pi$ interaction occurs between the ring R1 and Tyr435 (3.5 Å).

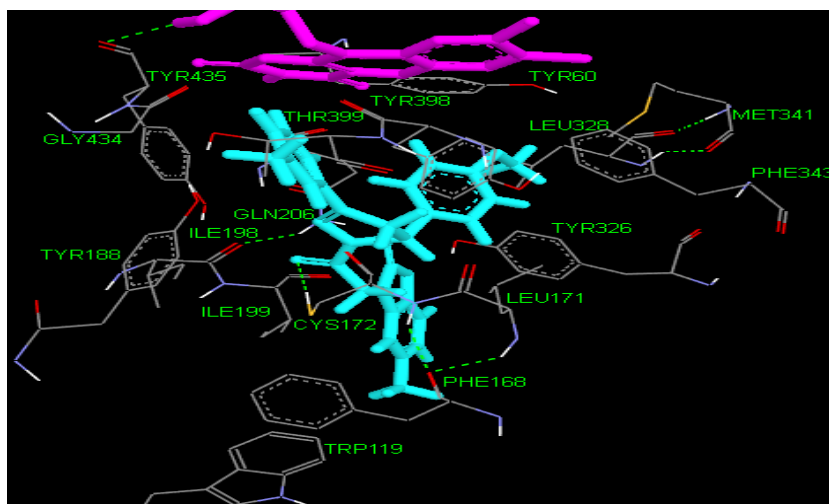


Figure 4.18. 3-D view of ligand 3b4r and active side of MAO-A at the lowest energy conformation. Pink color represent FAD compound, cyan color represent inhibitor, green dashed line represent hydrogen bonding.

Ligand 1c6s

Tyr435 makes two $\pi - \pi$ interactions (3.8 Å – 3.6 Å) with benzoxazolinone. Another $\pi - \pi$ interaction (6 Å) is obtained between Tyr188 and benzoxazolinone. On the other hand a cation - π interaction occurs between Cys172 and nitrogen atom of pyrazole. Gln206, Leu171, Ile198, Ile199 and Tyr326 are important residues where enclose to inhibitor.

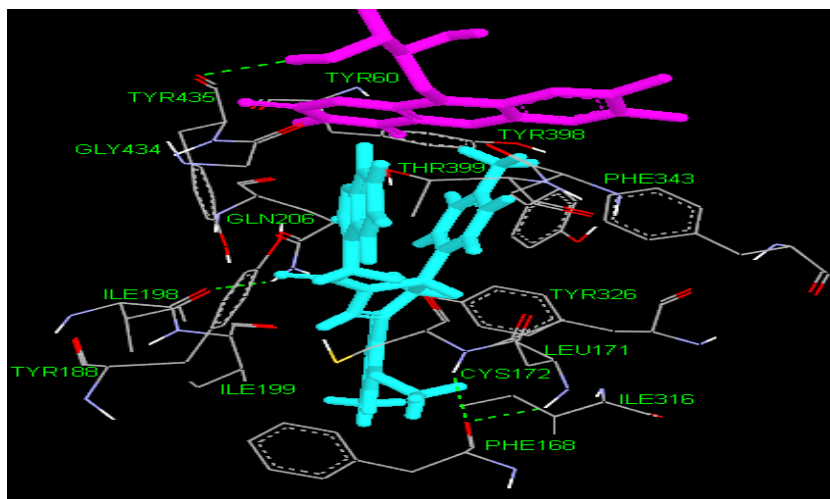


Figure 4.19. 3-D view of ligand 1c6s and active side of MAO-A at the lowest energy conformation. Pink color represent FAD compound, cyan color represent inhibitor, green dashed line represent hydrogen bonding.

Ligand 3d4s

When residues Tyr326, Leu171 are positioned close to ring R1, residues Phe343 and Tyr60 are positioned around the ring R2. Also residues Tyr188, Tyr435, Tyr398 are located close to benzoxazolinone ring. Other residues that surround the ligand are 3d4s, Thr399, Lys296, Gln206 and Gly434.

Tyr326 makes cation- π interaction (5.9Å) with nitrogen of pyrazole. Tyr188 makes π - π interaction (5.9 Å) with benzoxazolinone ring another π - π interaction occurs (3.9Å) between benzoxazolinone and Tyr435.

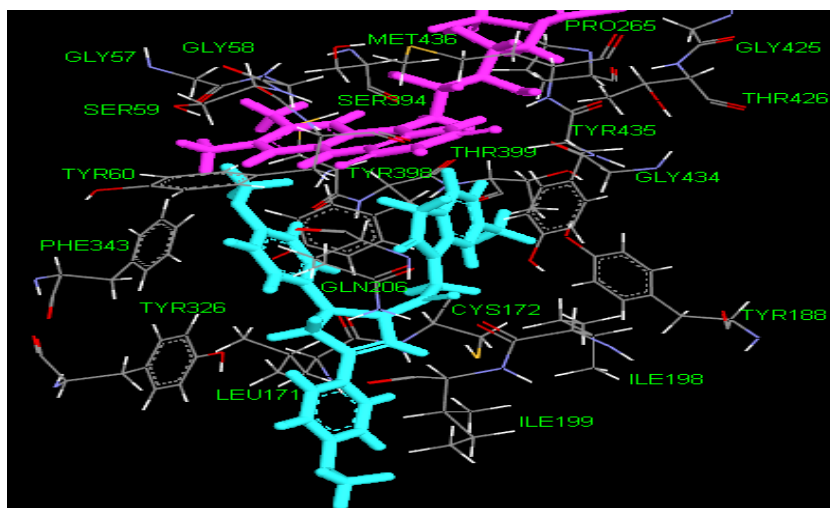
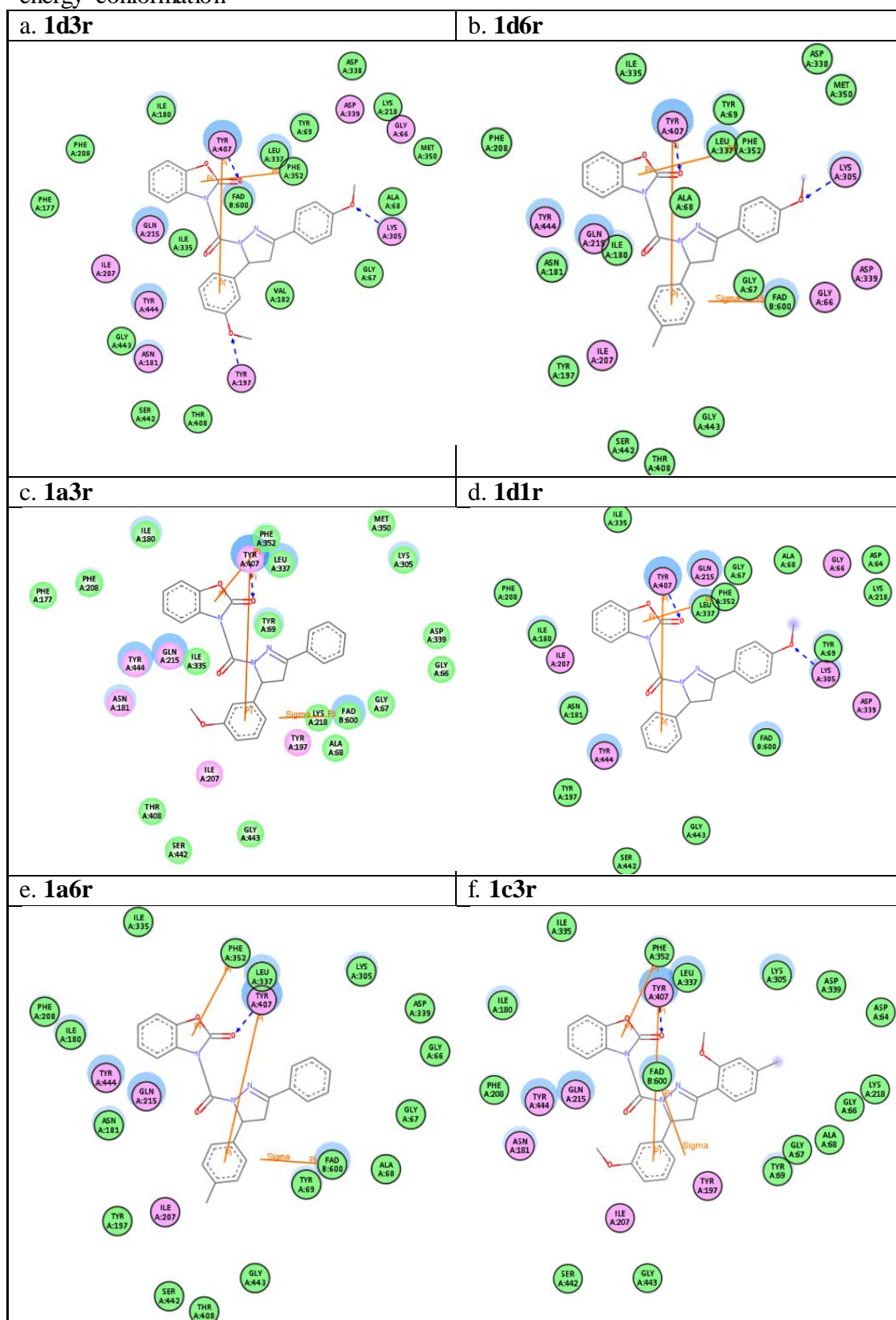


Figure 4.20. 3-D view of ligand 3d4s and active side of MAO-A at the lowest energy conformation. Pink color represent FAD compound, cyan color represent inhibitor, green dashed line represent hydrogen bonding.

Table 4.3. 2-D pictures of the ligands interaction by MAO-A at the lowest docking energy conformation



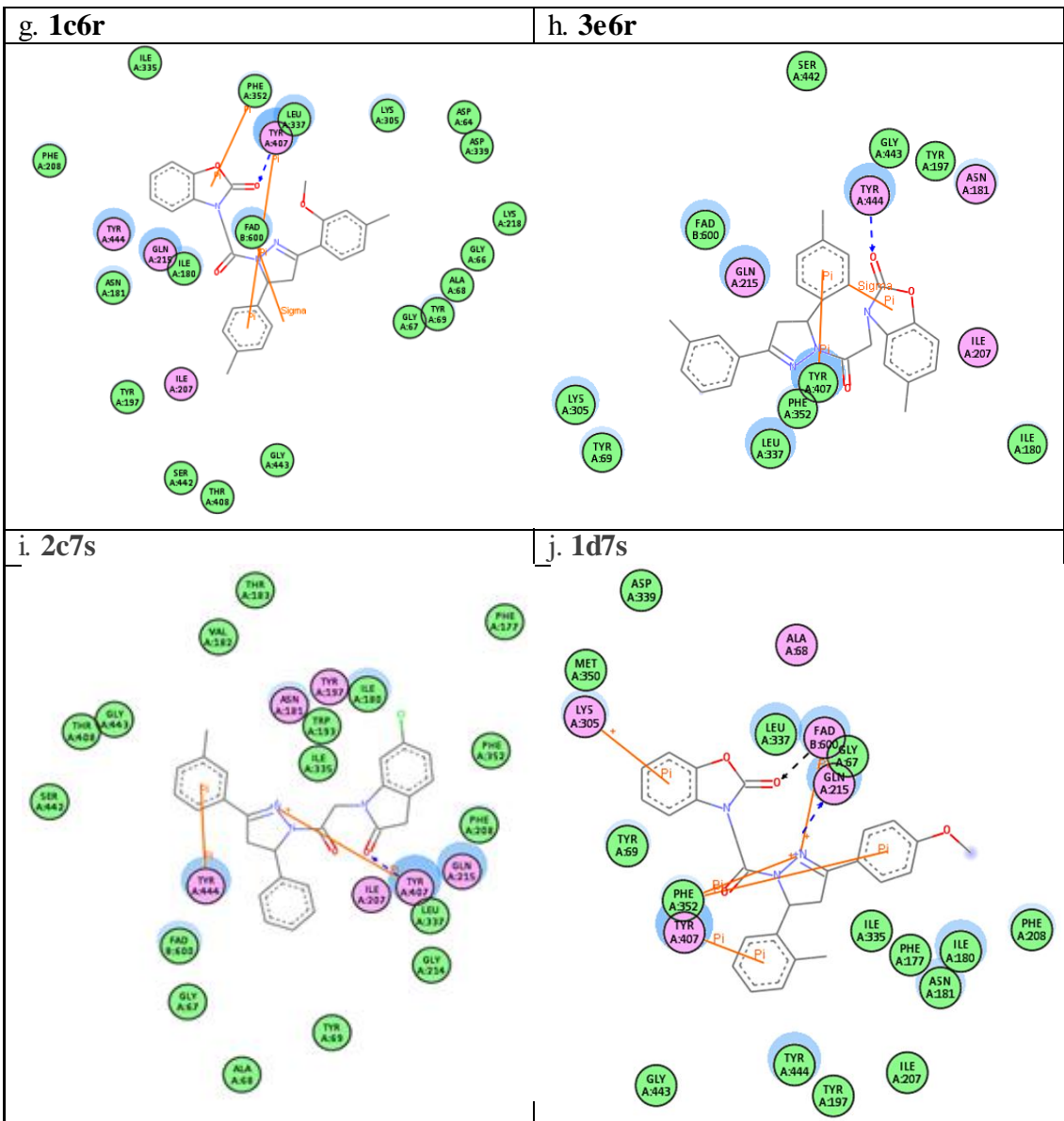
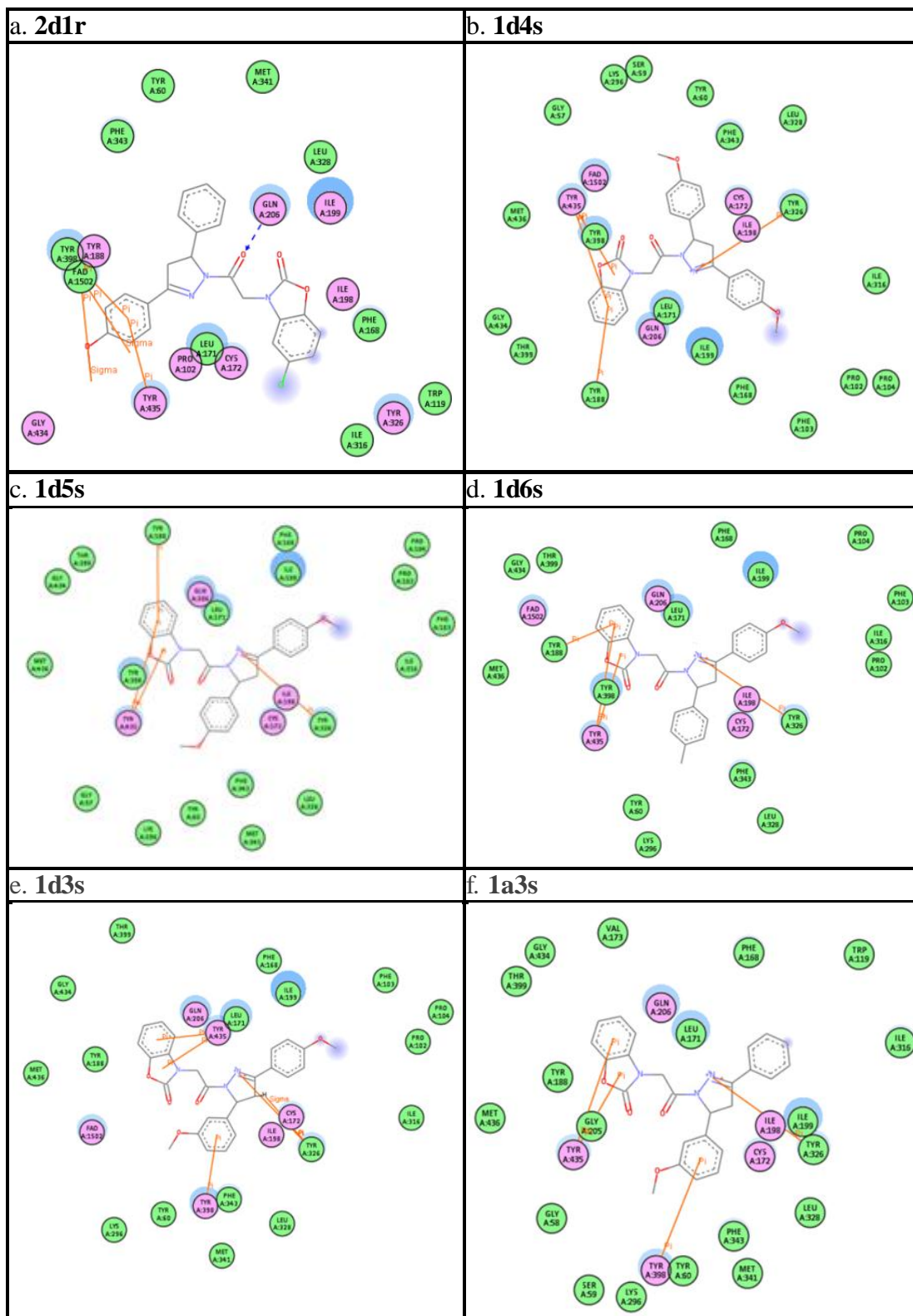
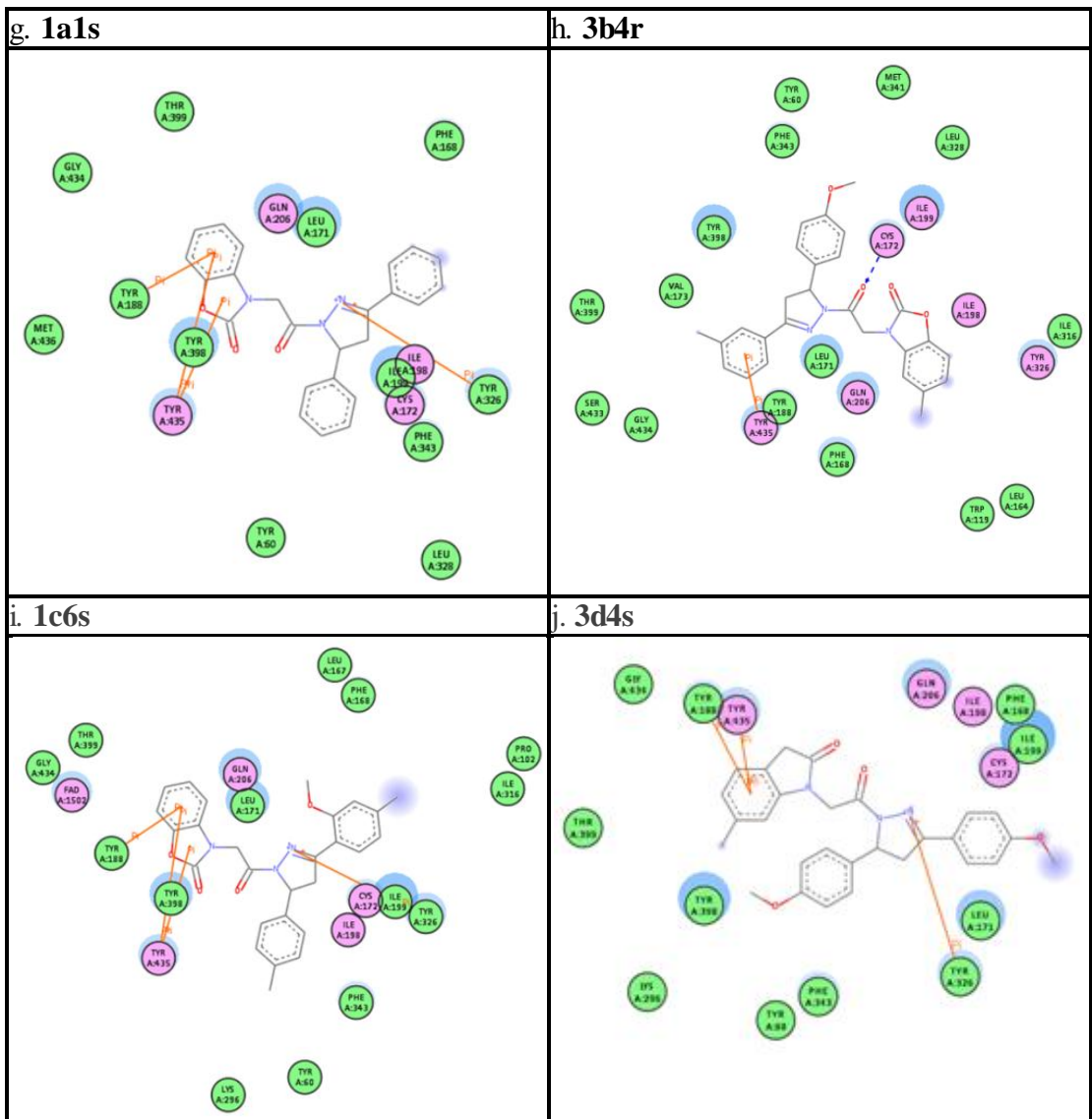


Table 4.4. 2-D pictures of the ligands interaction by MAO-B at the lowest docking energy conformation





Chapter 5

Conclusions

Considering recent studies and effective compounds, a lead scaffold is generated (4) and total 210 ligands that 105-r stereoisomers and 105-s stereoisomers are derived from this lead scaffold. Aim of this thesis, computer-aids inhibitor design for inhibition of both isozymes MAO-A and MAO-B. Each ligand is docked one by one with the using Autodock 4.2 and Accelrys 3.1 libdock tool. Each scoring function is based on different parameters for computation of docking simulations thus results are analyzed according to their significant scoring function instead correlation of all docking results.

After the docking studies by Autodock4.2 and Accelrys 3.1, binding free energy of autodock and libdock scores are obtained (Chapter 4). Autodock and libdock outputs are produced by their own special scoring functions. Thus, top ranking results of both docking studies are handled for comparing these results and determining probable drug candidates. General view for this study, when the ligands that have r-stereo isomers give much more effective score for MAO-A, other ligands that have s-stereo isomers give high ranking scores for MAO-B.

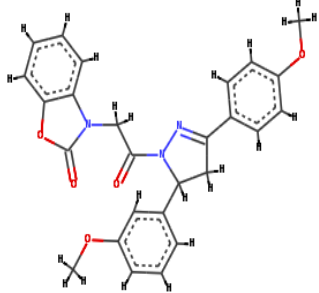
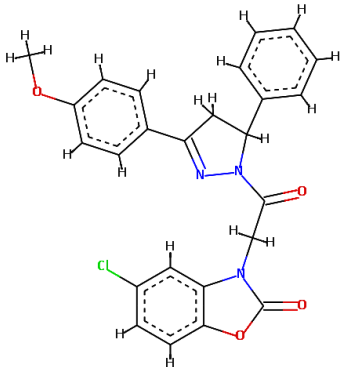
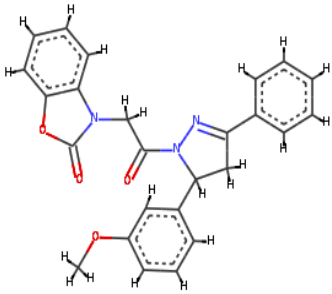
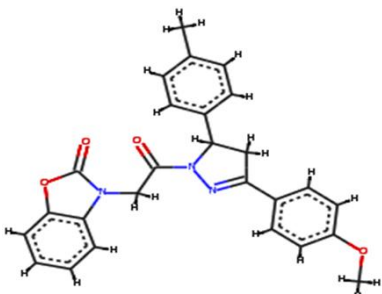
Analysis of MAO-A isozyme, docking results show a harmony for both docking tools. 1d3r exhibitions -13.09 kcal/mol lowest free binding energy and 90.79 libdock score for docking process so 1d3r is a considerable inhibitor candidate. Consider of the all ligands, MAO-A candidate inhibitors 1d1r and 1d3r - are substantially strong inhibition candidates. These two ligands has a common code d, so they have OCH₃ on the R1 ring. As analysis chapter 4, oxygen atom of OCH₃ makes hydrogen bounding with Lys305 for both candidates 1d3r and 1d1r. Another strong inhibitor candidates for MAO-A, have common a code such as 1a3r and 1a6r. Hence R1 ring has only hydrogen atoms are added as a result 1a3r makes sigma- π interaction by FAD and this plays a key role for a good candidate. Another

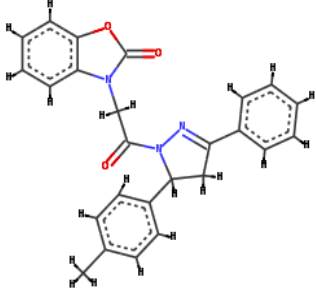
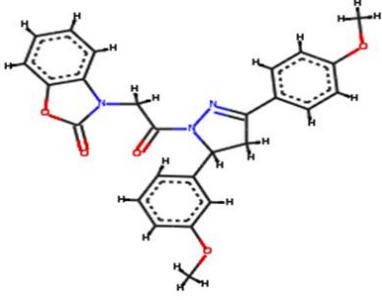
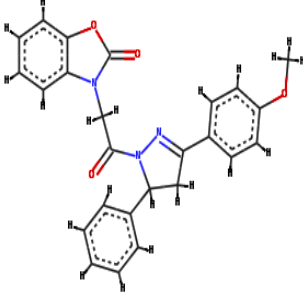
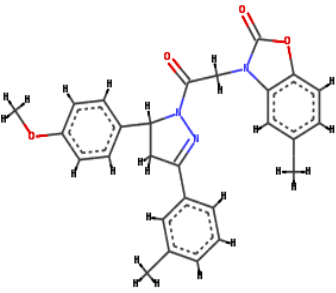
compound 1a3r displays 12.63 kcal/mol lowest free binding energy and 114.80 libdock score and as a result, 1a3r could be an effective MAO-A inhibitor. Other important inhibitor candidates are 1a6r and 1d1r. Examined to all MAO-A docking results, ligands which names start by code 1, gave better docking score than other ligands which names start by 2 and 3. Scilicet, ligands which have only hydrogen on the benzoxazolinone ring of scaffold (R) are more efficient for inhibition of MAO-A than other ligands such as names starting by 2 and 3. Respectively code 2 and 3 has chloride on the benzoxazolinone ring (R) and has methyl on the benoxazoinone ring (R). In addition, results of ligands which have methyl compound on the ring R1(second letter of code name is d) obviously display much better binding for both MAO isozymes such as 2d1r , 1d3r, 1d6r. We can generalize this situation for our most of ligands that performed by docking process.

On the other hand, inhibitor candidates of MAO-B isozyme prove effectual results according to docking studies. Also results of these inhibitor candidates display harmonious for both docking tools. 2d1r indicates -13.35 kcal/mol that lowest free binding energy and this is the best ranking for all docked ligand inhibitors. Also libdock score of 2d1r is observed as 140.8 so ligand 2d1r could be a great inhibitor for MAO-B. Another effective MAO-B inhibitor candidate is 1e6s. Lowest free binding energy of 1e6s is 11.61 kcal/mol and libdock score of 1d6s is 145.86. This libdock score is the best result between other candidate inhibitors of MAO-B. Other strong inhibitor candidates are found as 1d6s and 1d3s. As a result, ligands which target enzyme MAO-B are show effective results. Names starting with 1 are more effective docked exceptional ligands 2d1r and 3b4r. This situation shows, ligands that hydrogen on benzoxazolinone (R) gives better solution for inhibition of MAO-B than methyl or chloride on benzoxazolinone ring (R).

Detailed docking results and chemical structures of both isozymes, MAO-A and MAO-B inhibitor candidates are illustrated by in the table x.

Table.5.1 Detailed docking results and chemical structures of MAO-A and MAO-B inhibitor candidates are illustrated by in the table x.

| MAO-A Enzyme Candidates | | MAO-B Enzyme Candidates | |
|--|---|--|--|
| Inhibitor Candidates | Scaffold 2-D Structure | Inhibitor Candidates | Scaffold 2-D Structure |
| Name: 1d3r |  | Name: 2d1r |  |
| Autodock lowest free binding energy: -13.09 kcal/mol | | Autodock lowest free binding energy: -13.35 kcal/mol | |
| Libdock Score: 90.79 | | Libdock Score: 140.08 | |
| Name: 1a3r |  | Name: 1d6s |  |
| Autodock lowest free binding energy: -12.63 kcal/mol | | Autodock lowest free binding energy: -11.61 kcal/mol | |
| Libdock Score: 114.80 | | Libdock Score: 145.86 | |

| | | | |
|--|--|--|---|
| Name: 1a6r |  | Name: 1d3s |  |
| Autodock lowest free binding energy: -12.59 kcal/mol | | Autodock lowest free binding energy: -11.57 kcal/mol | |
| Libdock Score: 101.46 | | Libdock Score: 138.28 | |
| Name: 1d1r |  | Name: 3b4r |  |
| Autodock lowest free binding energy: -12.61 kcal/mol | | Autodock lowest free binding energy: -11.15 kcal/mol | |
| Libdock Score: 95.70 | | Libdock Score: 143.824 | |

According to this thesis study, ligands 1d3r, 1a3r and 1a6r could be used for inhibition of MAO-A isozyme and ligands 2d1r, 1e6s, 1e3s, 3c4r could be used for inhibition of MAO-B isoenzyme. We can suggest these scaffolds for design of new MAO inhibitors.

APPENDIX A: PARAMETER FILES of AUTODOCK 4.2 STUDIES

Grid parameter file of MAO-A docking

```
npts 80 80 80 # num.grid points in xyz
gridfld maoA_clean_prep.maps.fld # grid_data_file
spacing 0.375 # spacing(A)
receptor_types A C HD N NA O A P SA # receptor atom types
ligand_types A C N NA O A # ligand atom types
receptor maoA_clean_prep.pdbqt # macromolecule
gridcenter 33.625 30.159 -18.303 # xyz-coordinates or auto
smooth 0.5 # store minimum energy w/in rad(A)
map maoA_clean_prep.A.map # atom-specific affinity map
map maoA_clean_prep.C.map # atom-specific affinity map
map maoA_clean_prep.N.map # atom-specific affinity map
map maoA_clean_prep.NA.map # atom-specific affinity map
map maoA_clean_prep.OA.map # atom-specific affinity map
elecmap maoA_clean_prep.e.map # electrostatic potential map
dsolvmap maoA_clean_prep.d.map # desolvation potential map
dielectric -0.1465 # <0, AD4 distance-dep.diel;>0,
constant
```

Grid parameter file of MAO-B docking

```
npts 80 80 80 # num.grid points in xyz
gridfld 2v5z_mao_B__clean_prep.maps.fld # grid_data_file
spacing 0.375 # spacing(A)
receptor_types A C HD N NA O A P SA # receptor atom types
ligand_types A C N NA O A # ligand atom types
```

Appendix A

```
receptor 2v5z_mao_B__clean_prep.pdbqt # macromolecule
gridcenter 53.506 147.816 24.376 # xyz-coordinates or auto
smooth 0.5 # store minimum energy w/in rad(A)
map 2v5z_mao_B__clean_prep.A.map # atom-specific affinity map
map 2v5z_mao_B__clean_prep.C.map # atom-specific affinity map
map 2v5z_mao_B__clean_prep.N.map # atom-specific affinity map
map 2v5z_mao_B__clean_prep.NA.map # atom-specific affinity map
map 2v5z_mao_B__clean_prep.OA.map # atom-specific affinity map
elecmap 2v5z_mao_B__clean_prep.e.map # electrostatic potential map
dsolvmap # desolvation potential map
2v5z_mao_B__clean_prep.d.map
dielectric -0.1465 # <0, AD4 distance-dep.diel;>0,
constant
```

Docking parameter file of 1d3r and MAO-A docking

```
autodock_parameter_version 4.2 # used by autodock to validate
parameter set
outlev 1 # diagnostic output level
intelec # calculate internal electrostatics
seed pid time # seeds for random generator
ligand_types A C N NA OA # atoms types in ligand
fld maoA_clean_prep.maps.fld # grid_data_file
map maoA_clean_prep.A.map # atom-specific affinity map
map maoA_clean_prep.C.map # atom-specific affinity map
map maoA_clean_prep.N.map # atom-specific affinity map
map maoA_clean_prep.NA.map # atom-specific affinity map
map maoA_clean_prep.OA.map # atom-specific affinity map
elecmap maoA_clean_prep.e.map # electrostatics map
desolvmap maoA_clean_prep.d.map # desolvation map
move 1d3rf.pdbqt # small molecule
```

Appendix A

```
about -0.9233 1.5822 -0.0088      # center of small molecule
tran0 random                      # initial coordinates/A or random
axisangle0 random                 # initial orientation
dihe0 random                      # initial dihedrals (relative) or random
tstep 2.0                         # translation step/A
qstep 50.0                        # quaternion step/deg
dstep 50.0                        # torsion step/deg
torsdof 6                         # torsional degrees of freedom
rmstol 2.0                        # cluster_tolerance/A
extnrg 1000.0                    # external grid energy
e0max 0.0 10000                  # max initial energy; max number of
                                # retries
ga_pop_size 150                  # number of individuals in population
ga_num_evals 5000000             # maximum number of energy
                                # evaluations
ga_num_generations 27000         # maximum number of generations
ga_elitism 1                     # number of top individuals to survive
                                # to next generation
ga_mutation_rate 0.02           # rate of gene mutation
ga_crossover_rate 0.8           # rate of crossover
ga_window_size 10               #
ga_cauchy_alpha 0.0             # Alpha parameter of Cauchy
                                # distribution
ga_cauchy_beta 1.0              # Beta parameter Cauchy distribution
set_ga                           # set the above parameters for GA or
                                # LGA
sw_max_its 300                   # iterations of Solis & Wets local search
sw_max_succ 4                    # consecutive successes before
                                # changing rho
sw_max_fail 4                    # consecutive failures before changing
                                # rho
```

Appendix A

```
sw_rho 1.0 # size of local search space to sample
sw_lb_rho 0.01 # lower bound on rho
ls_search_freq 0.06 # probability of performing local search
                    on individual
set_psw1 # set the above pseudo-Solis & Wets
          parameters
unbound_model bound # state of unbound ligand
ga_run 50 # do this many hybrid GA-LS runs
analysis # perform a ranked cluster analysis
```

Docking parameter files of 2d1r and MAO-B docking

```
autodock_parameter_version 4.2 # used by autodock to validate
                                parameter set
outlev 1 # diagnostic output level
intelec # calculate internal electrostatics
seed pid time # seeds for random generator
ligand_types A C Cl N NA OA # atoms types in ligand
fld 2v5z_mao_B__clean_prep.maps.fld # grid_data_file
map 2v5z_mao_B__clean_prep.A.map # atom-specific affinity map
map 2v5z_mao_B__clean_prep.C.map # atom-specific affinity map
map 2v5z_mao_B__clean_prep.Cl.map # atom-specific affinity map
map 2v5z_mao_B__clean_prep.N.map # atom-specific affinity map
map 2v5z_mao_B__clean_prep.NA.map # atom-specific affinity map
map 2v5z_mao_B__clean_prep.OA.map # atom-specific affinity map
elecmap 2v5z_mao_B__clean_prep.e.map # electrostatics map
desolvmap # desolvation map
2v5z_mao_B__clean_prep.d.map
move 2d1rf.pdbqt # small molecule
about -3.1002 -0.1631 -0.0024 # small molecule center
tran0 random # initial coordinates/A or random
```

Appendix A

```
axisangle0 random          # initial orientation
dihe0 random              # initial dihedrals (relative) or random
tstep 2.0                 # translation step/A
qstep 50.0                # quaternion step/deg
dstep 50.0                # torsion step/deg
torsdof 5                 # torsional degrees of freedom
rmstol 2.0                # cluster_tolerance/A
extnrg 1000.0             # external grid energy
e0max 0.0 10000           # max initial energy; max number of
                           # retries
ga_pop_size 150           # number of individuals in population
ga_num_evals 5000000      # maximum number of energy
                           # evaluations
ga_num_generations 27000  # maximum number of generations
ga_elitism 1              # number of top individuals to survive
                           # to next generation
ga_mutation_rate 0.02    # rate of gene mutation
ga_crossover_rate 0.8    # rate of crossover
ga_window_size 10        #
ga_cauchy_alpha 0.0      # Alpha parameter of Cauchy
                           # distribution
ga_cauchy_beta 1.0       # Beta parameter Cauchy distribution
set_ga                    # set the above parameters for GA or
                           # LGA
sw_max_its 300            # iterations of Solis & Wets local
                           # search
sw_max_succ 4             # consecutive successes before
                           # changing rho
sw_max_fail 4             # consecutive failures before changing
                           # rho
sw_rho 1.0                # size of local search space to sample
```

Appendix A

```
sw_lb_rho 0.01 # lower bound on rho
ls_search_freq 0.06 # probability of performing local
                    search on individual
set_psw1 # set the above pseudo-Solis & Wets
          parameters
unbound_model bound # state of unbound ligand
ga_run 100 # do this many hybrid GA-LS runs
analysis # perform a ranked cluster analysis
```


APPENDIX B: RESULTS of AUTODOCK 4.2 DOCKING DATA

Table A.1 Results of the 210 ligand data set docked MAO-A enzyme

| Molecule Name | Average binding Free energy (kcal/mol) | Estimated Inhibition Constant (Ki) |
|---------------|--|------------------------------------|
| 1a1r | -10.5 | 20.11 nM |
| 1a1s | -11.48 | 3.87 nM |
| 1a2r | -11,25 | 5.72 nM |
| 1a2s | -11,06 | 7.86 nM |
| 1a3r | -12,63 | 550.71 pM |
| 1a3s | -11,73 | 2.52 nM |
| 1a4r | -11,86 | 2.03 nM |
| 1a4s | -11,01 | 8.54 nM |
| 1a5r | -11,69 | 2.71 nM |
| 1a5s | -8,98 | 263.11 nM |
| 1a6r | -12,59 | 589.50 pM |
| 1a6s | -11,17 | 6.53 nM |
| 1a7r | -12,02 | 1.54 nM |
| 1a7s | -11,32 | 5.06 nM |
| 1b1r | -11,91 | 1.86 nM |
| 1b1s | -11,29 | 5.31 nM |
| 1b2r | -9,58 | 94.88 nM |
| 1b2s | -9,35 | 140.95 nM |
| 1b3r | -11,41 | 4.32 nM |
| 1b3s | -11,22 | 6.01 nM |
| 1b4r | -11,62 | 3.01 nM |
| 1b4s | -9,76 | 69.84 nM |
| 1b5r | -11,53 | 3.51 nM |
| 1b5s | -8,23 | 924.46 nM |
| 1b6r | -12,16 | 1.23 nM |
| 1b6s | -10,34 | 26.46 nM |
| 1b7r | -11,17 | 6.45 nM |
| 1b7s | -10,81 | 12.02 nM |
| 1c1r | -11,97 | 1.69 nM |

| Molecule Name | Average binding Free energy (kcal/mol) | Estimated Inhibition Constant (Ki) |
|---------------|--|------------------------------------|
| 1c1s | -11,35 | 4.80 nM |
| 1c2r | -11,36 | 4.72 nM |
| 1c2s | -10,69 | 14.71 nM |
| 1c3r | -12,56 | 621.24 pM |
| 1c3s | -11,03 | 8.22 nM |
| 1c4r | -11,58 | 3.23 nM |
| 1c4s | -10,83 | 11.57 nM |
| 1c5r | -10,64 | 15.86 nM |
| 1c5s | -7,74 | 2.13 nM |
| 1c6r | -12,53 | 654.87 pM |
| 1c6s | -10,6 | 16.85 nM |
| 1c7r | -11,65 | 2.87 pM |
| 1c7s | -11,15 | 6.67 nM |
| 1d1r | -12,61 | 520.20 pM |
| 1d1s | -12,07 | 1.42 nM |
| 1d2r | -11,36 | 4.73 nM |
| 1d2s | -9,92 | 53.41 nM |
| 1d3r | -13,09 | 252.50 pM |
| 1d3s | -11,34 | 4.89 nM |
| 1d4r | -11,38 | 4.54 nM |
| 1d4s | -11,04 | 8.03 nM |
| 1d5r | -10,91 | 10.03 nM |
| 1d5s | -10,16 | 35.42 nM |
| 1d6r | -12,77 | 435.24 pM |
| 1d6s | -11,33 | 4.98 nM |
| 1d7r | -12,36 | 868.79 pM |
| 1d7s | -12,17 | 1.21 nM |
| 1e1r | -11,6 | 5.72 pM |
| 1e1s | -11,22 | 6.01 nM |

Appendix B

| Molecule Name | Average binding Free energy (kcal/mol) | Estimated Inhibition Constant (Ki) |
|---------------|--|------------------------------------|
| 1e2r | -11,69 | 2.71 nM |
| 1e2s | -11,4 | 4.44 nM |
| 1e3r | -13,02 | 283.75pM |
| 1e3s | -11,04 | 8.09 nM |
| 1e4r | -9,73 | 73.18 nM |
| 1e4s | -10,76 | 13.06 nM |
| 1e5r | -11,83 | 2.14 nM |
| 1e5s | -11,28 | 5.39 nM |
| 1e6r | -11,76 | 445.69pM |
| 1e6s | -10,65 | 15.54 nM |
| 1e7r | -12,65 | 532.92pM |
| 1e7s | -10,61 | 16.63 nM |
| 2a1r | -10,98 | 8.97 nM |
| 2a1s | -11,84 | 2.10 nM |
| 2a2r | -10,06 | 4.57 nM |
| 2a2s | -11,98 | 1.66 nM |
| 2a3r | -11,44 | 4.11 nM |
| 2a3s | -12,11 | 1.33 nM |
| 2a4r | -11,02 | 8.35 nM |
| 2a4s | -10,5 | 20.14 nM |
| 2a5r | -8,89 | 359.75nM |
| 2a5s | -11,69 | 2.68 nM |
| 2a6r | -11,47 | 3.88 nM |
| 2a6s | -11,65 | 2.87 nM |
| 2a7r | -10,8 | 12.07 nM |
| 2a7s | -12,61 | 568.89pM |
| 2b1r | -10,78 | 12.54 nM |
| 2b1s | -10,05 | 42.89 nM |
| 2b2r | -10,2 | 33.22 nM |
| 2b2s | -8,4 | 694.27nM |
| 2b3r | -9,85 | 60.34 nM |
| 2b3s | -9,91 | 54.77 nM |
| 2b4r | -10,2 | 33.14 nM |
| 2b4s | -10,37 | 24.91 nM |
| 2b5r | -10,35 | 25.80 nM |
| 2b5s | -10,78 | 12.59 nM |
| 2b6r | -10,49 | 20.56 nM |
| 2b6s | -10,15 | 36.05 nM |
| 2b7r | -11,1 | 7.28 nM |
| 2b7s | -10,74 | 13.48 nM |

| Molecule Name | Average binding Free energy (kcal/mol) | Estimated Inhibition Constant (Ki) |
|---------------|--|------------------------------------|
| 2c1r | -11,68 | 2.76 nM |
| 2c1s | -11,34 | 4.84 nM |
| 2c2r | -10,77 | 12.85 nM |
| 2c2s | -11,72 | 2.56 nM |
| 2c3r | -11,36 | 4.71 nM |
| 2c3s | -11,43 | 4.18 nM |
| 2c4r | -11,7 | 2.64 nM |
| 2c4s | -9,95 | 50.68 nM |
| 2c5r | -9,92 | 53.22 nM |
| 2c5s | -10,69 | 14.54 nM |
| 2c6r | -12,25 | 1.05 nM |
| 2c6s | -10,67 | 15.09 nM |
| 2c7r | -11,24 | 5.73 nM |
| 2c7s | -12,24 | 1.06 nM |
| 2d1r | -11,02 | 8.41 nM |
| 2d1s | -10,75 | 13.19 nM |
| 2d2r | -10,2 | 33.41 nM |
| 2d2s | -9,7 | 77.98 nM |
| 2d3r | -10,9 | 10.28 nM |
| 2d3s | -10,75 | 13.18 nM |
| 2d4r | -10,25 | 30.78 nM |
| 2d4s | -11,31 | 5.11 nM |
| 2d5r | -9,63 | 86.98 nM |
| 2d5s | -11,74 | 2.46 nM |
| 2d6r | -11,52 | 3.59 nM |
| 2d6s | -11,15 | 6.73 nM |
| 2d7r | -10,66 | 15.25 nM |
| 2d7s | -12,09 | 1.38 nM |
| 2e1r | -11,42 | 4.27 nM |
| 2e1s | -11,9 | 1.88 nm |
| 2e2r | -10,31 | 27.85 nM |
| 2e2s | -11,93 | 1.81 nM |
| 2e3r | -11,12 | 7.03 nM |
| 2e3s | -11,1 | 7.35 nM |
| 2e4r | -10,98 | 9.01 nM |
| 2e4s | -9,93 | 52.60 nM |
| 2e5r | -10,15 | 36.24 nM |
| 2e5s | -9,07 | 225.36nM |
| 2e6r | -11,46 | 3.95 nM |
| 2e6s | -10,17 | 35.11 nM |

Appendix B

| Molecule Name | Average binding Free energy (kcal/mol) | Estimated Inhibition Constant (Ki) |
|---------------|--|------------------------------------|
| 2e7r | -10,58 | 17.57 nM |
| 2e7s | -10,62 | 16.34 nM |
| 3a1r | -11,22 | 5.94 nM |
| 3a1s | -11,48 | 3.85 nM |
| 3a2r | -10,71 | 14.18 nM |
| 3a2s | -11,87 | 1.99 nM |
| 3a3r | -11,75 | 2.42 nM |
| 3a3s | -11,67 | 2.77 nM |
| 3a4r | -11,08 | 7.58 nM |
| 3a4s | -9,9 | 55.55 nM |
| 3a5r | -9,45 | 117.36nM |
| 3a5s | -10,53 | 19.10 nM |
| 3a6r | -11,62 | 3.05 nM |
| 3a6s | -11,4 | 4.37 nM |
| 3a7r | -11,26 | 5.58 nM |
| 3a7s | -12,2 | 1.15 nM |
| 3b1r | -10,93 | 9.74 nM |
| 3b1s | -10,11 | 38.82 nM |
| 3b2r | -11,03 | 8.16 nM |
| 3b2s | -9,99 | 47.49 nM |
| 3b3r | -11,23 | 5.90 nM |
| 3b3s | -9,54 | 102.41 nM |
| 3b4r | -10,93 | 9.79 nM |
| 3b4s | -11,16 | 6.55 nM |
| 3b5r | -9,57 | 95.84 nM |
| 3b5s | -10,78 | 12.54 nM |
| 3b6r | -11,09 | 7.46 nM |
| 3b6s | -11,21 | 6.05 nM |
| 3b7r | -10,6 | 16.99 nM |
| 3b7s | -10,33 | 26.62 nM |
| 3c1r | -11,8 | 2.24 nM |
| 3c1s | -11,24 | 5.77 nM |
| 3c2r | -10,82 | 11.74 nM |
| 3c2s | -10,81 | 11.96 nM |
| 3c3r | -11,66 | 2.86 nM |
| 3c3s | -11,02 | 8.35 nM |

| Molecule Name | Average binding Free energy (kcal/mol) | Estimated Inhibition Constant (Ki) |
|---------------|--|------------------------------------|
| 3c4r | -12,18 | 1.17 nM |
| 3c4s | -10,37 | 25.18 nM |
| 3c5r | -10,77 | 12.71 nM |
| 3c5r | -11,49 | 3.81 nM |
| 3c6r | -11,82 | 2.17 nM |
| 3c6s | -11,69 | 2.70 nM |
| 3c7r | -11,23 | 5.85 nM |
| 3c7s | -11,91 | 1.86 nM |
| 3d1r | -11,73 | 2.51 nM |
| 3d1s | -11,59 | 3.17 nM |
| 3d2r | -10,42 | 22.97 nM |
| 3d2s | -11,68 | 2.74 nM |
| 3d3r | -12,32 | 931.54 pM |
| 3d3s | -11,34 | 4.90 nM |
| 3d4r | -11,8 | 2.24 nM |
| 3d4s | -9,95 | 50.52 nM |
| 3d5r | -10,73 | 13.69 nM |
| 3d5s | -10,58 | 17.65 nM |
| 3d6r | -11,61 | 3.08 nM |
| 3d6s | -11,42 | 4.29 nM |
| 3d7r | -11,18 | 6.38 nM |
| 3d7s | -12,28 | 990.9 pM |
| 3e1r | -11,69 | 2.69 nM |
| 3e1s | -12,04 | 1.50 nM |
| 3e2r | -10,33 | 26.96 nM |
| 3e2s | -11,95 | 1.74 nM |
| 3e3r | -12,23 | 1.09 nM |
| 3e3s | -10,81 | 11.85 nM |
| 3e4r | -11,65 | 2.91 nM |
| 3e4s | -10,15 | 36.27 nM |
| 3e5r | -10,97 | 9.08 nM |
| 3e5s | -11,4 | 4.37 nM |
| 3e6r | -12,38 | 848.42 pM |
| 3e6s | -11,49 | 3.81 nM |
| 3e7r | -11,23 | 5.87 nM |
| 3e7s | -12,28 | 990.17 pM |

Table A.2 Results of the 210 ligand data set docked Mao-B enzyme

| Molecule Name | Average binding Free energy (kcal/mol) | Estimated Inhibition Constant (Ki) |
|---------------|--|------------------------------------|
| 1a1r | -8.68 | 432.24 nM |
| 1a1s | -11.16 | 6.60 nM |
| 1a2r | -8.79 | 359.66 nM |
| 1a2s | -8.75 | 385.28 nM |
| 1a3r | -9.71 | 75.91 nM |
| 1a3s | -11.35 | 4.79 nM |
| 1a4r | -9.9 | 55.72 nM |
| 1a4s | -10.2 | 33.25 nM |
| 1a5r | -6.74 | 11.40 μM |
| 1a5s | -9.66 | 82.84 nM |
| 1a6r | -8.42 | 667.82 nM |
| 1a6s | -9.57 | 95.87 nM |
| 1a7r | -9.32 | 146.39 nM |
| 1a7s | -9.83 | 62.81 nM |
| 1b1r | -8.72 | 405.88 nM |
| 1b1s | -10.15 | 36.50 nM |
| 1b2r | -7.38 | 3.89 μM |
| 1b2s | -6.13 | 32.09 μM |
| 1b3r | -8.6 | 492.91 nM |
| 1b3s | -9.24 | 167.75 nM |
| 1b4r | -9.42 | 124.69 nM |
| 1b4s | -10.43 | 22.46 nM |
| 1b5r | -6.5 | 17.23 μM |
| 1b5s | -5.91 | 46.56 μM |
| 1b6r | -9.54 | 101.08 nM |
| 1b6s | -9.65 | 84.66 nM |
| 1b7r | -7.96 | 1.45 μM |
| 1b7s | -9.73 | 74.24 nM |
| 1c1r | -9.16 | 193.68 nM |
| 1c1s | -10.41 | 23.39 nM |
| 1c2r | -8.35 | 758.33 nM |
| 1c2s | -10.35 | 25.71 nM |
| 1c3r | -8.9 | 298.12 nM |
| 1c3s | -10.17 | 35.18 nM |
| 1c4r | -9.21 | 177.04 nM |
| 1c4s | -10.48 | 20.96 nM |
| 1c5r | -5.93 | 44.83 μM |
| 1c5s | -9.36 | 137.91 nM |

| Molecule Name | Average binding Free energy (kcal/mol) | Estimated Inhibition Constant (Ki) |
|---------------|--|------------------------------------|
| 1c6r | -8.45 | 635.52 nM |
| 1c6s | -11.13 | 6.96 nM |
| 1c7r | -7.7 | 2.27 μM |
| 1c7s | -9.33 | 143.98 nM |
| 1d1r | -9.73 | 73.37 nM |
| 1d1s | -8.84 | 328.80 nM |
| 1d2r | -8.51 | 576.77 nM |
| 1d2s | -10.59 | 17.21 nM |
| 1d3r | -9.7 | 77.62 nM |
| 1d3s | -11.11 | 7.15 nM |
| 1d4r | -9.76 | 64.91 nM |
| 1d4s | -11.69 | 2.69 nM |
| 1d5r | -6.62 | 14.02 μM |
| 1d5s | -11.63 | 2.97 nM |
| 1d6r | -11.61 | 231.66 nM |
| 1d6s | -11.42 | 242.95 nM |
| 1d7r | -8.65 | 453.60 nM |
| 1d7s | -10.75 | 13.20 nM |
| 1e1r | -9.38 | 134.13 nM |
| 1e1s | -11.62 | 3.02 nM |
| 1e2r | -8.51 | 582.64 nM |
| 1e2s | -10.44 | 22.14 nM |
| 1e3r | -9.67 | 81.83 nM |
| 1e3s | -11.57 | 3.30 nM |
| 1e4r | -7.87 | 1.71 μM |
| 1e4s | -8.99 | 257.23 nM |
| 1e5r | -9.8 | 65.18 nM |
| 1e5s | -10 | 47.07 nM |
| 1e6r | -9.02 | 4.26 nM |
| 1e6s | -9.05 | 3.09 nM |
| 1e7r | -8.18 | 1.01 μM |
| 1e7s | -9.77 | 68.56 nM |
| 2a1r | -9.24 | 169.75 nM |
| 2a1s | -8.97 | 266.43 nM |
| 2a2r | -7.84 | 1.80 μM |
| 2a2s | -8.97 | 264.60 nM |
| 2a3r | -7.48 | 3.30 μM |
| 2a3s | -10.33 | 26.83 nM |

Appendix B

| Molecule Name | Average binding Free energy (kcal/mol) | Estimated Inhibition Constant (Ki) |
|---------------|--|------------------------------------|
| 2a4r | -8 | 1.37 μ M |
| 2a4s | -9.66 | 82.86 nM |
| 2a5r | -7.04 | 6.86 μ M |
| 2a5s | -6.9 | 8.69 μ M |
| 2a6r | -7.9 | 1.62 μ M |
| 2a6s | -9.65 | 84.68 nM |
| 2a7r | -8.9 | 298.97 nM |
| 2a7s | -9.11 | 211.75 nM |
| 2b1r | -9.31 | 149.71 nM |
| 2b1s | -9.5 | 108.83 nM |
| 2b2r | -6.83 | 9.92 μ M |
| 2b2s | -6.62 | 14.02 μ M |
| 2b3r | -7.31 | 4.38 μ M |
| 2b3s | -7.78 | 2.00 μ M |
| 2b4r | -7.67 | 2.39 μ M |
| 2b4s | -9.48 | 113.29 nM |
| 2b5r | -6.5 | 17.30 μ M |
| 2b5s | -6.57 | 15.31 μ M |
| 2b6r | -8.36 | 750.04 nM |
| 2b6s | -9.1 | 212.98 nM |
| 2b7r | -8.28 | 857.31 nM |
| 2b7s | -9.47 | 113.59 nM |
| 2c1r | -9.45 | 118.87 nM |
| 2c1s | -9.95 | 50.96 nM |
| 2c2r | -7.48 | 3.26 μ M |
| 2c2s | -8.55 | 539.21 nM |
| 2c3r | -8.99 | 258.01 nM |
| 2c3s | -10.5 | 20.00 nM |
| 2c4r | -8.61 | 485.78 nM |
| 2c4s | -10.4 | 23.69 nM |
| 2c5r | -6.36 | 21.84 μ M |
| 2c5s | -7.7 | 2.28 μ M |
| 2c6r | -8.35 | 757.64 nM |
| 2c6s | -10.37 | 24.99 nM |
| 2c7r | -7.97 | 1.44 μ M |
| 2c7s | -8.02 | 1.32 μ M |
| 2d1r | -13.35 | 165.01 pM |
| 2d1s | -9.89 | 56.66 nM |
| 2d2r | -6.8 | 10.28 μ M |
| 2d2s | -6.45 | 18.75 μ M |

| Molecule Name | Average binding Free energy (kcal/mol) | Estimated Inhibition Constant (Ki) |
|---------------|--|------------------------------------|
| 2d3r | -9.14 | 200.53 nM |
| 2d3s | -10.1 | 39.41 μ M |
| 2d4r | -5.56 | 83.43 μ M |
| 2d4s | -8.42 | 673.97 μ M |
| 2d5r | -6.13 | 32.29 μ M |
| 2d5s | -10.19 | 33.69 nM |
| 2d6r | -8.89 | 302.48 nM |
| 2d6s | -9.81 | 63.93 μ M |
| 2d7r | -7.51 | 3.15 μ M |
| 2d7s | -7.99 | 1.40 μ M |
| 2e1r | -9.68 | 80.49 nM |
| 2e1s | -10.32 | 27.35 nM |
| 2e2r | -7.79 | 1.94 μ M |
| 2e2s | -8.4 | 698.75 nM |
| 2e3r | -9.25 | 166.92 nM |
| 2e3s | -10.62 | 16.42 nM |
| 2e4r | -8.54 | 551.32 nM |
| 2e4s | -10.33 | 26.98 nM |
| 2e5r | -6.05 | 36.86 μ M |
| 2e5s | -8.71 | 415.83 nM |
| 2e6r | -8.87 | 314.39 nM |
| 2e6s | -10.04 | 43.37 nM |
| 2e7r | -8.63 | 471.19 nM |
| 2e7s | -7.62 | 2.61 μ M |
| 3a1r | -9.25 | 166.78 nM |
| 3a1s | -10.16 | 35.57 nM |
| 3a2r | -7.75 | 2.10 μ M |
| 3a2s | -8.04 | 1.27 μ M |
| 3a3r | -8.22 | 936.19 nM |
| 3a3s | -10.14 | 36.71 nM |
| 3a4r | -8.75 | 388.63 nM |
| 3a4s | -10.45 | 21.84 nM |
| 3a5r | -6.99 | 7.53 μ M |
| 3a5s | -7.83 | 1.82 μ M |
| 3a6r | -8.19 | 998.28 nM |
| 3a6s | -10.44 | 22.09 nM |
| 3a7r | -8.6 | 495.56 nM |
| 3a7s | -8.77 | 374.59 nM |
| 3b1r | -9.09 | 216.34 nM |
| 3b1s | -9.52 | 104.50 nM |

Appendix B

| Molecule Name | Average binding Free energy (kcal/mol) | Estimated Inhibition Constant (Ki) |
|---------------|--|------------------------------------|
| 3b2r | -8.1 | 1.16 μ M |
| 3b2s | -6.33 | 22.91 μ M |
| 3b3r | -8.15 | 1.05 μ M |
| 3b3s | -8.79 | 363.22 nM |
| 3b4r | -11.15 | 6.77 nM |
| 3b4s | -9.63 | 86.73 nM |
| 3b5r | -6.52 | 16.75 μ M |
| 3b5s | -7.78 | 1.99 μ M |
| 3b6r | -8.41 | 682.34 nM |
| 3b6s | -10.01 | 45.80 nM |
| 3b7r | -8.42 | 675.59 nM |
| 3b7s | -6.78 | 10.80 μ M |
| 3c1r | -9.35 | 140.83 nM |
| 3c1s | -10.13 | 37.46 nM |
| 3c2r | -7.21 | 5.17 μ M |
| 3c2s | -8.59 | 509.15 nM |
| 3c3r | -9.69 | 79.00 nM |
| 3c3s | -10.3 | 28.41 nM |
| 3c4r | -7.32 | 4.33 μ M |
| 3c4s | -11.01 | 8.54 nM |
| 3c5r | -6.49 | 17.36 μ M |
| 3c5s | -6.49 | 17.39 μ M |
| 3c6r | -8.7 | 418.46 nM |
| 3c6s | -11.08 | 7.52 nM |
| 3c7r | -8.8 | 356.24 nM |
| 3c7s | -8.49 | 595.30 nM |
| 3d1r | -9.16 | 192.27 nM |

| Molecule Name | Average binding Free energy (kcal/mol) | Estimated Inhibition Constant (Ki) |
|---------------|--|------------------------------------|
| 3d1s | -10.4 | 23.62 nM |
| 3d2r | -8.42 | 669.28 nM |
| 3d2s | -9.29 | 155.77 nM |
| 3d3r | -9.05 | 231.11 nM |
| 3d3s | -10.41 | 23.36 nM |
| 3d4r | -8.9 | 301.59 nM |
| 3d4s | -10.71 | 14.13 nM |
| 3d5r | -5.01 | 212.28 μ M |
| 3d5s | -8.61 | 484.44 nM |
| 3d6r | -8.36 | 742.87 nM |
| 3d6s | -10.47 | 21.21 nM |
| 3d7r | -8.79 | 359.18 nM |
| 3d7s | -7.96 | 1.45 μ M |
| 3e1r | -9.61 | 91.04 nM |
| 3e1s | -10.97 | 9.11 nM |
| 3e2r | -8.1 | 1.15 μ M |
| 3e2s | -9.01 | 248.68 nM |
| 3e3r | -9.92 | 53.43 nM |
| 3e3s | -10.76 | 12.96 nM |
| 3e4r | -9.08 | 221.02 nM |
| 3e4s | -10.8 | 12.04 nM |
| 3e5r | -6.04 | 37.09 μ M |
| 3e5s | -7.31 | 4.35 μ M |
| 3e6r | -8.7 | 419.04 nM |
| 3e6s | -10.83 | 11.58 nM |
| 3e7r | -8.22 | 936.44 nM |
| 3e7s | -8.67 | 440.60 nM |

Bibliography

- [1] Bortalato, M., Chen, K., and Shih, J.C., The degradation of Serotonin: Role of MAO. In C. P. Müller and B. L. Jacobs (Eds.), *Handbook of the behavioral neurobiology of serotonin* (pp.203-218). San Diego, CA:Elsevier.
- [2] Richards, J. G., Saura, J., Ulrich, J., and Prada, M.D. (1992). Molecular neuroanatomy of monoamine oxidases in human brainstem. *Journal of Psychopharmacology*,106, 21-23.
- [3] Şimşek, Ö.Ö. (2009),*Hekzahidroindazoltürevleri üzerinde çalışmalar*. *Unpublished master's thesis*, University of Hacettepe, Ankara.
- [4] Shi L., Yang Y., Li Z. L., Zhu Z. W., Liu C. H., and Zhu H. L. (2010). Design of novel nicotinamides as potent and selective monoamine oxidase a inhibitors. *Bioorganic & Medicinal Chemistry*, 18(4),1659-1664.
- [5] Yelekçi, K., Karahan, Ö., and Toprakçı M. (2007) “Docking of novel reversible monoamine oxidase-B inhibitors: efficient prediction of ligand binding sites and estimation of inhibitors thermodynamic properties. *Journal of Neural Transmission*, 114, 725-732.
- [6] Chimenti F., Fioravanti R., Bolasco A., Chimenti P., Secci D., Rossi F., Yáñez M., Orallo F., Ortusa F., Alcaro S., Cirilli R., Feretti R., and Sanna M. L. (2010). A new series of flavones, thioflavones, and flavonones as selective monoamine oxidase-B. *Bioorganic & Medicinal Chemistry*,18(3), 1273-1279.

- [7] Son S. Y., Ma J., Kondou Y., Yoshimura M., Yamashita E., and Tsukihara T.(2008). Structure of human monoamine oxidase A at 2.2-Å resolution: The central of opening the entry for substrates/inhibitors. *Proceedings of The National Academy of Science*, 105(15), 5739-5744 doi:10.1073/pnas.0710626105
- [8] Oak J., N., Hubert H., M., and Van T.(2008). Dopamine system. In S. Offermanns and W. Rosenthal (Eds.), *Encyclopedia of Molecular Pharmacology*, (pp. 437-442). New York, NY:Springer-Verbeg.
- [9] Kuchel, O. G., and Kuchel, G. A. (1991). Peripheral dopamine in pathophysiology of hypertension interaction with aging and lifestyle. *Hypertension Journal of the American heart association*,18(6), 709-721.
- [10] Edmondson, D. E., Binda, C., and Mattevi, A. (2004). The FAD binding sites of human monoamine oxidases A and B. *Neuro Toxicology* 25(1-2),63-72
- [11] European Bioinformatics Institute. *Avarage mass and formula of dopamine*. Retrieved August 5, 2010, from <http://www.ebi.ac.uk/chebi/searchId.do?chebiId=18243>
- [12] College of Pharmacy University of Texas. *Dopamine-A sample neurotransmitter*. Retrieved, Januvary, 2010 from <http://www.utexas.edu/research/asrec/dopamine.html>
- [13] Morón J. A., Brockington A., Wise R. A., Rocha B. A., and Hope B. T. (2002). Dopamine uptake through the norepinephrine transporter in brain regions low levels of the dopamine transporter: evidence *from* knock-out mouse lines *Journal of Psychiatry and Neuroscience*, 22(2), 389-395
- [14] Young, S. N. (2007). How to increase serotonin in the human brain without drugs. *Journal of Psychiatry and Neuroscience*, 32(6), 394-395.

- [15] Byrd, A. (2002) *Serendip of Bryn Mawr College*. Retrived January 07, 2002, from <http://serendip.brynmawr.edu/bb/neuro/neuro99/web1/Byrd.html>
- [16] St. Edward's university school of natural sciences. *Monoamine Oxidase*. Retrived July 18, 2005, from <http://www.cs.stedwards.edu/chem/Chemistry/CHEM43/CHEM43/AmineOxidases/function.htm>
- [17] Cannon, W.B. (1929). Emotion. In H.Wagner and K. Siber (Eds.), *Physiological Psychology* (pp.185-189) Available from <http://books.google.com/>
- [18] Lehninger, A. L., Nelson D. L. and Cox, M. M. (2004). *Lehninger principles biochemistry*. (Fourth edition). In A. L. Lehninger (Eds.), (pp. 908) New York, NY:Freeman
- [19] National center of biotechnology information. *Norepinephrine compound*. Retrieved September 16, 2004, from <http://pubchem.ncbi.nlm.nih.gov/summary/summary.cgi?cid=439260>
- [20] Guyton A. C. and Hall J. E. (2006). *Textbook of medical physiology. Rhythmical excitation of the heart (pp.111-117)* Philadelphia, PA:Elsevier Inc
- [21] Yu, J. (1998). *Synthesis and mechanistic studies on the mononamine oxidase (MAO) catalyzed oxidation of 1,4-disubstituted-1,2,3,6-tetrahydropyridines*. Virginia Polytechnic Institute and State University, Petersburg.
- [22] Erdem, S. S., Karahan Ö., Yıldız İ. and Yelekçi K. (2006). A computational study on the amine-oxidation mechanism of monoamine oxidase: Insight into the polar nucleophilic mechanism, *Organic & Biomolecular Chemistry*, 4, 646-658.

[23] Akyüz, M. A. (2007). *Monoamin oksidaz substratlarının enzim aktif bölgesi içinde QM/MM yöntemi ile modellenmesi. Unpublished master's thesis, University of Marmara, Istanbul*

[24] Çiğit A. K. (2005). *Mononamin oksidaz inhibisyonu ile ilişkili model amin bileşiklerinin konformasyonel analizi. Unpublished master's thesis, University of Marmara, Istanbul*

[25] Cutler, D. M. (2004). Your money or your life: strong medicine for America's Healthcare system. *The power of the pill prozac and the revolution in mental health care. (pp.32-46), NewYork NY:Oxford University Press*

[26] Maxwell, R. A., and Eckhardt, S. B. (1990). Drug discovery: a casebook and analysis.(first edition) (pp.455). New York, NY:Humana Press

[27] Nair, N. P., Ahmed, S. K., and Kin, N.N. (1993). Biochemistry and pharmacology of reversible inhibitors of MAO-A agents: focus on moclobemide. *Journal of Psychiatry and Neuroscience, 18(5), 214-25.*

[28] New Zealand medicines and medical devices safety authority. *Moclobemide*. Retrieved June 16, 2010, from <http://www.medsafe.govt.nz/profs/datasheet/g/genrxmoclobemidetab.pdf>

[29] Heritage T. W. (2003) Protein structure: determination, analysis and applications for drug discovery. In D. I. Chasman (Eds.). *Molecular docking in structure based design. (pp. 417-452)*. New York NY:Marcel Dekker Inc

[30] The Scripps Research Institute.*Autodock*. Retrieved August 08, 2001, from <http://autodock.scripps.edu/>

[31] Accelrys Software Inc. *Discovery studio structure based design* , Retrieved July 02, 2011, from <http://accelrys.com/products/discovery-studio>

[32] Accelrys Software Inc. *Discovery studio 2.5 bridging modern methods and validated science*, Retrieved July 14, 2009 from <http://www.accelryskorea.com/download/@100610-KUGM/ds01.pdf>

[33] Son S. Y., Ma J., Kondou Y., Yoshimura M., Yamashita E., and, Tsukihara T. (2008). Crystal structure of human monoamine oxidase A with harmine. *Proceedings of The National Academy of Sciences*, 105(15), 5739-5744. doi: 10.1073/pnas.0710626105

[34] Binda C., Wang J., Pisani L., Caccia C., Carotti A., Salvati P., Edmondson D. E., and, Mattevi A. (2007). Structure of human MAO B in complex with the selective inhibitor safinamide. *Journal of Medicinal Chemistry*, 50(23), 5848–5852. doi: 10.1021/jm070677y

Curriculum Vitae

Çağla Mıdık was born on 10 April 1985, in Kütahya. He qualify for his BS degree in Science and Technology in Education Faculty at Marmara University and in 2009 and M.S. degree in 2012 in Computational Biology and Bioinformatics from Kadir Has University. He worked as a science and technology teacher at the primary school of Şeyhli and primary school of Çubuklu. from 2010 to 2012. During this time he has been affiliated with the Educational Volunteers Foundation of Turkey. Contact, email; caglamidik@gmail.com